https://doi.org/10.5194/egusphere-2026-2497
Preprint. Discussion started: 26 June 2026

Systematic Analysis of Rain-on-Snow Events and Their Trends in the French Alps: Distinguishing All and Impactful Events across Mountain Ranges

Paul Fournier[1], Antoine Blanc[2], Juliette Blanchet[3], and Matthieu Lafaysse[4]

[1]École polytechnique, Palaiseau, France
[2]RTM-ONF, Grenoble, France
[3]IGE, Univ. Grenoble Alpes, CNRS, IRD, INRAE, Grenoble-INP, Grenoble, France
[4]Univ. Grenoble Alpes, Université de Toulouse, Météo-France, CNRS, CNRM, Centre d'études de la Neige, Grenoble, France

Correspondence: Paul Fournier (paul.fournier.2022@polytechnique.org) and Juliette Blanchet (juliette.blanchet@univ-grenoble-alpes.fr)

Abstract. Rain-on-snow (ROS) events are a major hydrometeorological phenomenon in mountainous regions, as the combination of liquid precipitation and snowmelt enhances flood hazard. This study provides the first systematic analysis of ROS events in the French Alps at high temporal and spatial resolution, based on the S2M reanalysis (1958–2024) with an hourly time step. By combining meteorological data with an event database of torrential floods and landslides, ROS events are explicitly linked to observed impacts. Averaged over space, 5.5 ROS events occurred per year in the French Alps over 1958–2024, with a clear contrast between the more frequently affected north-western mountain ranges and the south-eastern ones. Seasonality strongly depends on elevation, with ROS events occurring mainly in winter at lower elevations and in spring at higher elevations. Impactful ROS events, associated with torrential floods or landslides, are characterized by high cumulative rainfall and long durations. Above 76 mm of cumulative rainfall, the probability that a ROS event is impactful exceeds 50 $\%$, defining heavy-rainfall ROS events. Trend analyses reveal a marked decline in overall ROS occurrence (-22 $\%$) between 1959–1988 and 1995–2024, primarily in spring and early summer due to a shortening of the snow season, while increases are observed in December and January as precipitation more frequently falls as rain. Heavy-rainfall ROS events show a more moderate decrease (-9 $\%$), with declining trends in most southern mountain ranges but increases in several northern ones. They now predominantly occur in early winter at lower elevations, which are more densely populated, making them more likely to produce damaging impacts. The next step in this systematic approach would be to create a watershed-based subdivision of the French Alps to enable comprehensive hydrological analyses of ROS events.

1 Introduction

Rain-on-snow (ROS) events combine liquid precipitation falling on a snow-covered surface that is often close to saturation, with concurrent snowmelt. This results in a total runoff that exceeds the rainfall amount alone, thereby increasing flood hazard (Singh et al., 1997; Würzer et al., 2016). Alpine regions are particularly exposed to such processes, with sometimes severe consequences, as illustrated by the floods in the Bernese Alps on 10 October 2011 (Rössler et al., 2014) and the destruction

https://doi.org/10.5194/egusphere-2026-2497
Preprint. Discussion started: 26 June 2026

of the Saint-Hilaire funicular in the French Alps on 29 December 2021 (Strizzolo et al., 2023). Improving the understanding of ROS events is therefore necessary to develop protection strategies for the safety of populations living in mountain regions. Over the past 25 years, numerous studies have investigated ROS events at mid and high latitudes (Table 1). While several contributions have focused on the Swiss Alps, ROS events have not yet been the subject of a dedicated, systematic analysis over the French Alps.

The characterization of ROS events requires information on both precipitation occurrence and phase, as well as their timing relative to snowpack conditions. Consequently, long-term observations of precipitation and air temperature at high temporal resolution are particularly valuable for accurately identifying and characterizing ROS events. However, such data sets remain scarce in mountain regions and their availability decreases with elevation. In our study area (Sect. 2.1), while some monitoring networks provide up to four decades of hourly precipitation measurements, the simultaneous availability of precipitation and temperature records is much more limited: only five stations above 750 m of elevation provide at least 30 years of complete data, and no station above 2100 m offers more than 20 years of continuous measurements. Most previous studies have therefore relied on daily time step data (Table 1) which imposes two major limitations. First, the identification of precipitation phase – already a complex issue in itself (Casellas et al., 2021; Froidurot et al., 2014; Jennings et al., 2018) – ignores the frequently high sub-daily variability in precipitation phase, introducing uncertainties in the detection of ROS events. Second, event duration cannot be properly estimated, and events are often associated with calendar days, leading to inaccuracies when events span multiple days. The recent availability of hourly data sets over several decades, particularly from reanalysis products, now enables a more realistic definition of meteorological events, with durations ranging from a few hours to several days. However, detailed ROS analyses at hourly resolution remain scarce (e.g., Katz et al., 2023; Würzer et al., 2016).

Despite their limited temporal resolution, previous studies have established a robust body of knowledge regarding ROS occurrence characteristics and trends under a warming climate. At mid-latitudes, ROS events primarily occur between October and May (Freudiger et al., 2014; McCabe et al., 2007). Their seasonality strongly depends on elevation, with two main occurrence modes (McCabe et al., 2007; Morán-Tejeda et al., 2016). In winter, ROS events primarily affect lower elevations, where snow cover is intermittent and rainfall is frequent, whereas in late spring and early summer, they occur at higher elevations, where snow accumulated during winter persists while temperatures rise. No clear annual-scale trend in ROS occurrence emerges over the Northern Hemisphere as a whole (Cohen et al., 2015). However, when distinguishing by season and elevation, the literature consistently reports a decrease in spring–summer ROS events (Beniston and Stoffel, 2016; Freudiger et al., 2014; Morán-Tejeda et al., 2016; Pall et al., 2019) associated with a shortening of the snow season (Morán-Tejeda et al., 2016; Pall et al., 2019), and an increase in winter at elevations where snow cover remains present (McCabe et al., 2007; Beniston and Stoffel, 2016; Freudiger et al., 2014; Morán-Tejeda et al., 2016; Musselman et al., 2018). Quantitatively, however, reported characteristics and trends vary widely depending on event definitions, regions, and elevation ranges.

Importantly, not all ROS events lead to natural hazards. Purely meteorological analyses therefore provide limited insight into the actual risks associated with ROS. To address this limitation, some studies focus on events exceeding high rainfall thresholds (e.g. 20 mm in Beniston and Stoffel (2016) ; 50 mm in Würzer et al. (2016)). Many works assess hydrological responses using runoff models. They highlighted the importance of initial snowpack properties such as liquid water content, density, and cold

https://doi.org/10.5194/egusphere-2026-2497
Preprint. Discussion started: 26 June 2026

Table 1. Overview of data, rainfall (RF) thresholds, event durations, regions, and periods covered in ROS studies.

Reference	Data type	Time step	RF	Duration	Region	Period
Sui and Koehler (2001)	Observations	daily	–	1 to 3 days	Northern Danube, Germany	1961–1995
McCabe et al. (2007)	Observations	daily	–	1 day	Western United States	1949–2003
Ye et al. (2008)	Observations	6 h then 3 h	–	1 day	Northern Eurasia (Russia)	1936–1990
Freudiger et al. (2014)	Interpolated observations (E-OBS)	daily	≥ 3 mm	1 to 6 days	Germany	1950–2011
Cohen et al. (2015)	MERRA reanalysis	daily	≥ 10 mm	1 day	Northern Hemisphere	1979–2014
Beniston and Stoffel (2016)	Observations and snowMAUS hydrological model	daily	≥ 50 mm	1 day	Sitter River catchment, Switzerland	1960–2015
Morán-Tejeda et al. (2016)	Observations and RCM for projections	daily	≥ 5 mm	1 day	Switzerland	1972–2012
Würzer et al. (2016)	Observations, RhiresD reanalysis and SNOWPACK hydrological model	hourly	≥ 20 mm	1 h to no limit	Swiss Alps	1998–2014
Musselman et al. (2018)	WRF reanalysis	daily	≥ 10 mm	1 day	Western North America	2000–2013
Li et al. (2019)	Interpolated observations and VIC hydrological model	daily	≥ 3 mm	1 day	United States	1950–2013
Pall et al. (2019)	Interpolated observations (seNorge) and NVE hydrological model	daily	≥ 5 mm	1 day	Norway	1957–2016
Katz et al. (2023)	Observations and SNOWPACK hydrological model	hourly	≥ 5 mm	1 h to 9 days	Independence Creek, California	1981–2019
Bonsoms et al. (2024)	SAFRAN reanalysis and FS2M hydrological model	hourly	≥ 10 mm	1 day	Pyrenees, France & Spain	1980–2019

content (Würzer et al., 2016; Katz et al., 2023). However, these modeling results are rarely confronted with observed impacts. Event-based analyses linked to documented disasters remain scarce and are generally limited to individual case studies (e.g. Rössler et al., 2014).

This work contributes to the literature by addressing the aforementioned gaps. We provide the first systematic analysis of ROS events in the French Alps. Using the S2M reanalysis, this work is high-resolution: it is at the scale of mountain ranges and at an hourly time step over the 1958–2024 period. While a reanalysis provides a spatially complete and temporally consistent framework, its gridded nature implies a spatial averaging of meteorological conditions that may not fully capture local-scale processes in complex mountainous terrain. Moreover, long-term trends derived from reanalyses may be affected by temporal heterogeneities in the assimilated observations. To address this issue, S2M-derived ROS characteristics are compared with available station observations. We further combine the meteorological analysis with the RTM event database, which documents natural hazard events in the French Alps. This unique coupling allows us to identify ROS events associated with damaging floods or landslides. The following terminology is therefore adopted in this study:

- ROS event: a meteorological occurrence characterized by liquid precipitation falling on an existing snowpack (Sect. 3.1).
- Impactful ROS event: a ROS event that has triggered one or more natural hazard events registered in the RTM database (Sect. 3.3).
- Heavy-rainfall ROS event: a ROS event with total rainfall exceeding 76 mm (Sect. 3.4).

https://doi.org/10.5194/egusphere-2026-2497
Preprint. Discussion started: 26 June 2026

By distinguishing between all ROS events and impactful ROS events, this study bridges a major gap in the existing literature. Specifically, we aim to answer the following questions: What are the main characteristics and trends of ROS events in the French Alps? To what extent do ROS events contribute to natural hazard impacts in this region? Are the observed trends in ROS event occurrence different between impactful events and other events?

The study area and data sets are presented in Sect. 2. The definition of ROS events, the variables analyzed, and the methodology used to link meteorological events with natural hazard records are described in Sect. 3. Results are organized into a comparison with observation stations (Sect 4.1), an assessment of mean characteristics over 1958–2024 (Sect. 4.2) and an analysis of observed trends over the same period (Sect. 4.3), systematically distinguishing between all ROS events and impactful ones. The results are discussed in Sect. 5.

2 Data

2.1 Study Area

This study focuses on the French Alps, located in southeastern France. The exact study area is defined by the geometry of the S2M reanalysis (Vernay et al., 2022) data set (Fig 1a). It encompasses 23 mountain ranges (hereafter referred to as *massifs*) and partly overlaps seven French administrative departments : Haute-Savoie, Savoie, Isère, Drôme, Hautes-Alpes, Alpes-de-Haute-Provence, and Alpes-Maritimes, as shown in Fig 1b. The considered elevations range from 750 m, below which snow cover is assumed to be negligible, to 3150 m, above which no meteorological observations are available within our study area. Figure 1b shows the location of the observation stations within the study area, which were used for comparison with S2M results.

2.2 S2M Reanalysis

S2M (Vernay et al., 2022) is a meteorological and snow cover reanalysis covering the French Alps, the Pyrenees, and Corsica. The acronym S2M refers to the numerical chain (SAFRAN, SURFEX/ISBA–Crocus, and MEPRA) historically developed to study the climatic variability of meteorological and snow conditions over the French mountains. SAFRAN (Durand et al., 1993) provides hourly meteorological analyzes by combining numerical weather models (ERA-40 reanalysis (Uppala et al., 2005) and the French global prediction model ARPEGE, both at a 6-hour resolution) with available in situ meteorological observations. These hourly data drive SURFEX/ISBA–Crocus (Vionnet et al., 2012; Lafaysse et al., 2017), which simulates the thermodynamic evolution of the snowpack layers. S2M provides the precipitation phase as a binary variable (rain or snow), without a fractional liquid/solid partition. It is first determined from the 0 °C isotherm elevation and subsequently adjusted using ground observations to ensure consistency with the observed daily proportion of solid precipitation (Vernay et al., 2022).

The reanalysis outputs are provided for each massif and different elevation bands. A massif corresponds to a mountain area within which meteorological conditions are assumed to only vary with elevation; their mean area is about 1000 km^2. The French Alps are divided into 23 such massifs (Fig 1a). The vertical resolution is 300 m, with the upper (resp. lower) band limit defined as the nearest multiple of 300 m above (resp. below) the highest (lowest) point of the massif. Elevation bands are

https://doi.org/10.5194/egusphere-2026-2497
Preprint. Discussion started: 26 June 2026

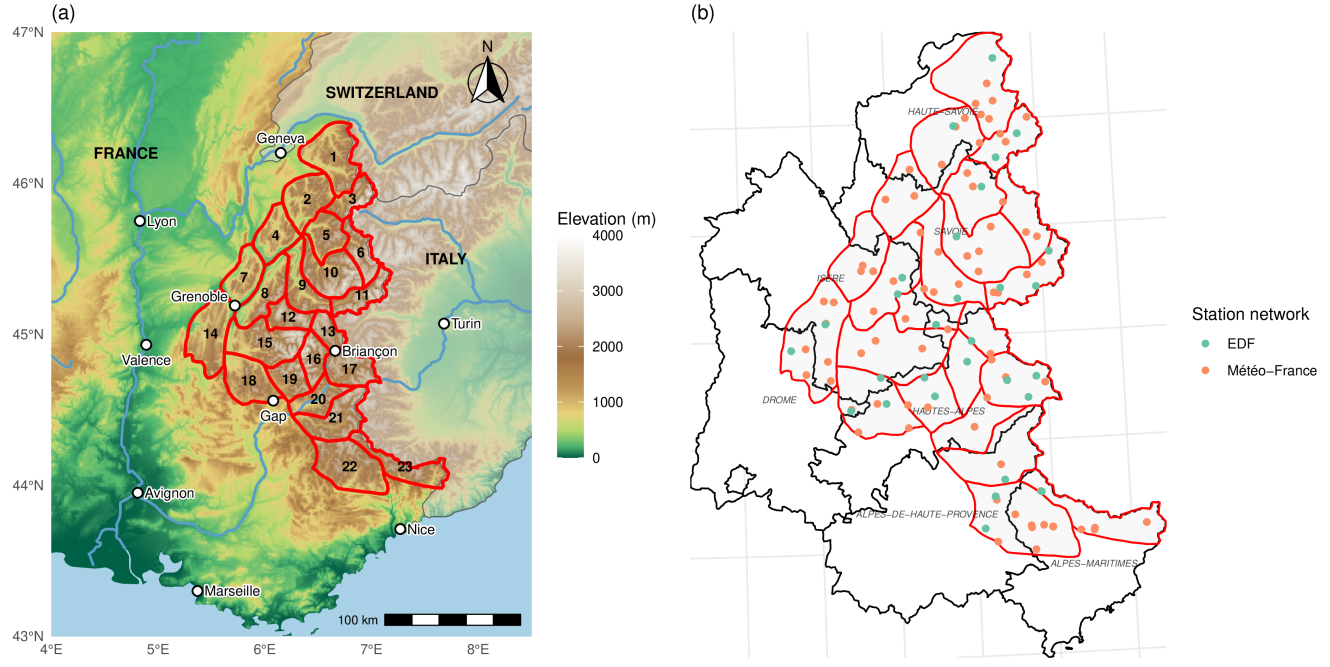

Figure 1. Map of the study area. (a) French Alpine massifs as defined in the S2M reanalysis. Elevation data: AWS Terrain Tiles (derived from SRTM, GMTED2010, and other public elevation datasets). (b) Observation stations within the S2M massifs used for comparison, along with the contours of administrative departments. Station coverage across the massifs is relatively dense and homogeneous.
Massifs in (a) are numbered as follows: 1 Chablais; 2 Aravis; 3 Mont-Blanc; 4 Bauges; 5 Beaufortain; 6 Haute-Tarentaise; 7 Chartreuse; 8 Belledonne; 9 Maurienne; 10 Vanoise; 11 Haute-Maurienne; 12 Grandes-Rousses; 13 Thabor; 14 Vercors; 15 Oisans; 16 Pelvoux; 17 Queyras; 18 Devoluy; 19 Champsaur; 20 Parpaillon; 21 Ubay; 22 Haut-Var–Haut-Verdon; 23 Mercantour.

referred to by their mean elevation (e.g. the 900 m band corresponds to elevations between 750 and 1150 m). For snow cover simulations, the full data set also distinguishes eight slope orientations (N, NE, E, SE, S, SW, W, NW) and two slope angles (20° and 40°). For this study, the "flat" S2M data set – i.e. without distinction of slope aspect or angle – was used as the RTM event database (Sect. 2.4) employed for coupling is also "flat". The study covers the 1958–2024 period, snow years starting on 1 August at 06:00 UTC. Meteorological variables are provided at an hourly time step, while snowpack variables are available daily. The daily resolution of the snowpack data is not limiting here, as it is used solely to define the binary presence or absence of snow on the ground, for which intra-daily variability is low. The S2M variables used in this study to identify ROS events (Sect. 3.1) include hourly liquid precipitation, as well as daily snow depth and snow water equivalent simulated at 06:00 UTC.

The use of this reanalysis greatly facilitates processing compared to station-based observations, avoiding missing data and ensuring a consistent temporal framework across the entire study domain. However, caution is required when analyzing long-term trends, which may be affected by temporal heterogeneities in the assimilated observations, as shown by Vernay et al. (2022). This is addressed by comparing S2M ROS event results with observation stations (Sect. 4.1).

https://doi.org/10.5194/egusphere-2026-2497
Preprint. Discussion started: 26 June 2026

2.3 Observation Stations

Observation stations are used only to evaluate ROS event results obtained from the S2M reanalysis system (Sect. 4.1). As S2M already assimilates station data (Sect. 2.2), this comparison tests whether ROS event results depend on spatial scale, i.e. massif-scale averages versus point-based observations. All other analyses presented in this study rely on S2M data.

Two observation networks were used: Météo-France stations and those operated by the French national electric power company *Électricité de France* (EDF). 80 Météo-France and 29 EDF stations were selected based on the following criteria: location within an S2M massif, elevation above 750 m, and at least one complete year – i.e. less than 15 $\%$ of missing data – of hourly precipitation and air temperature records. Their locations are shown in Fig. 1b. The data sets follow internal quality-control procedures; therefore, no additional processing was applied to the hourly precipitation totals. To reduce biases associated with instrumentation changes or shelter modifications, air temperature time series were homogenized against the Météo-France long-term homogenized series (LSH) (Moisselin et al., 2002). The homogenization script, developed by EDF, is based on the *Standard Normal Homogeneity Test* (SNHT; Alexandersson (1986)), see Appendix A. Precipitation phase at stations was inferred from air temperature (T_a) using a threshold of $T_a = 0.9$ °C, selected as the closest representation of the rain–snow distinction applied in S2M, see Appendix B. Since direct snow observations are sparse and often unavailable at station locations, snow depth and snow water equivalent were extracted from S2M to identify ROS events (Sect. 3.1) at the stations.

2.4 RTM Event Database

The *restauration des terrains en montagne* (RTM, restoration of mountain land) service of the National Forest Office (ONF), in charge of managing and preventing natural hazards in French mountainous regions, is the primary observer of natural hazard events occurring in these areas. Natural hazard events are defined here as phenomena producing observable impacts such as damage, disruptions, or geomorphological changes. The recording of such events began at the departmental level around 1980 as an internal database. In 2001, event documentation became an official mission funded by the French Ministry for the Environment (Bisquert et al., 2025), leading to the formal creation of the RTM event database (hereafter referred to as the RTM-DB).

The RTM-DB currently catalogs seven types of natural hazard events: avalanches (A), gullies or erosional processes (E), subsidence (F), floods (I), landslides (G), rockfalls (P), and torrential floods (T). Each event is assigned an intensity level from 1 to 4 based on its physical magnitude or impacts. Events are linked to a geographical site – ranging from a small hamlet or torrent channel to an entire municipality – and are described through several manually completed fields, such as event type, known or assumed causes, duration, impacts (casualties, damage, disruptions), and witness accounts. Data are entered by RTM field officers, primarily sector managers, and validated by thematic experts who ensure the internal consistency of records within each event type (Bisquert et al., 2025). Historical research and field investigations have also been conducted to enrich the database with older events dating back to the ninth century.

https://doi.org/10.5194/egusphere-2026-2497
Preprint. Discussion started: 26 June 2026

While manual input allows for detailed qualitative information, it limits large-scale statistical analysis. The progressive structuring of the RTM-DB between 1980 and 2001 introduces a temporal bias: since the system became an official mission of the RTM in 2001, event reporting has become more systematic, whereas earlier events are likely underrepresented. A sharp increase in the number of recorded events during the 1990s probably reflects improved reporting rather than an actual rise in natural phenomena (Creutin et al., 2022). Geographical biases may also exist. Despite standardized national protocols, the organization and practices of departmental RTM offices differ, as do the sensitivity and availability of individual field officers, particularly for low-intensity events. The manual nature of event descriptions can also affect data quality, as the causes are often multiple and not directly observed. Finally, the RTM-DB is not exhaustive; it relies on human observation and reporting, making it anthropocentric. Areas with high population density and infrastructure exposure tend to record more events, whereas remote high-elevation areas are poorly monitored. Increasing human presence in mountain regions may thus introduce additional temporal bias. Consequently, there is no direct relationship between the number of RTM-DB events and the number of meteorological episodes. All the more so, since a single meteorological episode can trigger several events (e.g., multiple torrential floods). Despite these limitations, the RTM-DB is the best available data set to investigate the links between natural events and impacts over the French Alps.

3 Methods

3.1 ROS Event Definition

The criteria used to define ROS events were chosen to remain consistent with those used in the literature (Table 1). The threshold on total rainfall (*RF*) was set relatively low in order to capture all ROS events. A distinction between all and high-rainfall (impact-prone) ROS events is made later in the event-based analysis. For snow cover conditions, the thresholds on snow depth (*SD*) and snow water equivalent (*SWE*) were set in the upper range of the literature to avoid detecting events for which the possible contribution of snow melt is insignificant. Taking advantage of the hourly time step, ROS events were defined with variable durations, from one hour to unlimited. Following the approach of Würzer et al. (2016), the start and end of an event are determined by a moving-window threshold on accumulated rainfall. To account for successive episodes occurring quickly, a minimum separation of 12 hours was imposed between events. The applied definition is summarized below, and an example time series is shown in Fig 2.

- $SD \geq 10$ cm and $SWE \geq 10$ mm at the beginning of the event (values from the nearest 06:00 UTC S2M simulation);
- Start: $RF \geq 3$ mm over 12 h;
- End: $RF < 3$ mm over 12 h;
- Total $RF \geq 5$ mm over the event;
- At least 12 h between two events.

https://doi.org/10.5194/egusphere-2026-2497
Preprint. Discussion started: 26 June 2026

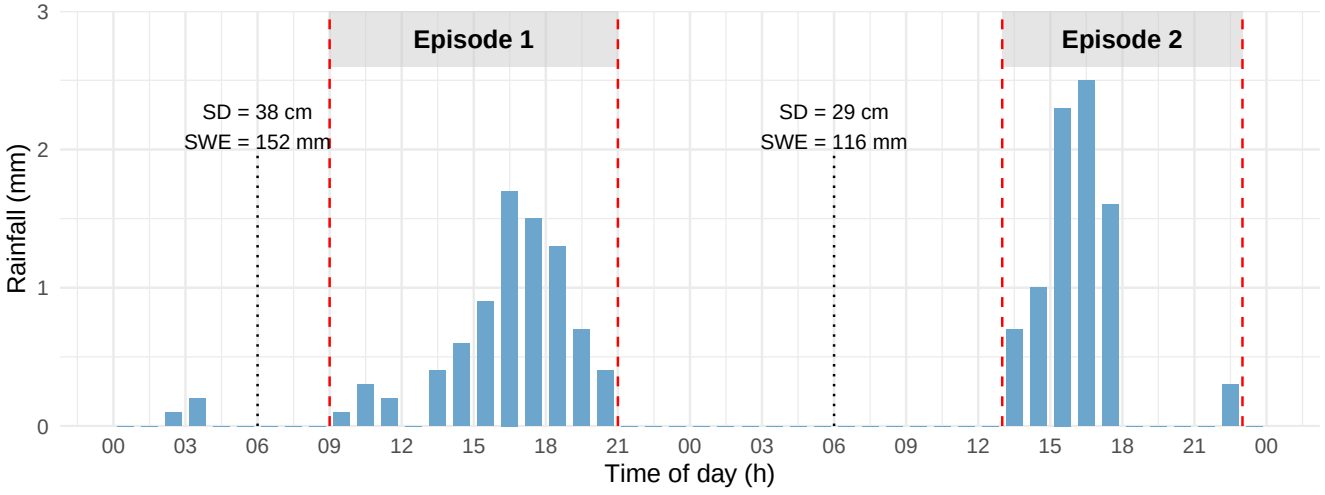

Figure 2. Example time series of ROS events.

3.2 Studied Variables and Spatial Scales

Three variables were analyzed to characterize ROS events: (1) their frequency of occurrence, expressed as the number of events per year (years are defined from 1 August to 31 July, consistent with the snow year convention used in S2M); (2) the total rainfall per event (mm); and (3) the event duration (h). These variables were computed at different spatial scales: over the entire French Alps, by massif, by elevation band, and by massif–elevation combination. Since S2M data are provided at the massif and elevation-band scale, larger-scale results were obtained by averaging. The massifs and elevation bands do not represent equal surface areas; to account for this, event frequencies were area-weighted. Specifically, the number of events in each massif–elevation unit was multiplied by its surface area, then normalized by the total area of the considered region (French Alps, massif, or elevation band). Throughout this study, unless otherwise stated, the numbers of ROS events are always area-weighted means. For total rainfall per event and event duration, simple (unweighted) averages were applied. Conceptually, this approach is equivalent to assigning a single representative value to a large spatial cell composed of heterogeneous sub-units. Weighting by area ensures that larger surfaces contribute proportionally more to the aggregated metric, avoiding biases toward small regions. From a statistical perspective, the resulting area-weighted mean can be interpreted as the expected number of events that would be observed at a randomly chosen location within the considered region. The massifs have relatively similar surface areas, so the weighting mainly applies to the elevation bands. Its primary effect is to reduce the relative contribution of the two highest bands (2700 m and 3000 m). The surface areas were derived from a 10 m resolution digital elevation model.

3.3 RTM ROS Event Selection and Impactful ROS Event Definition

For the event-based analysis, three types of natural hazard events were selected: torrential floods (T), floods (I), and landslides (G). These types were chosen because they are the most likely to be triggered by ROS conditions. This selection is not overly

https://doi.org/10.5194/egusphere-2026-2497
Preprint. Discussion started: 26 June 2026

restrictive, as T and G events are the two most frequently recorded types in the Isère department (Bisquert et al., 2025). Avalanche events were not considered since some recorded avalanches are human-triggered, accidentally or preventively, and thus cannot be reliably attributed to ROS conditions.

Natural hazard events caused by ROS were identified in two steps. First, an automatic preselection was performed based on the keywords "*neige*" (snow), "*fonte*" (snowmelt), and "*redoux*" (warm spell), searched across all available descriptive fields. Then, each preselected record was manually reviewed, mainly using the fields describing the nature of the phenomenon and its causes. Some uncertainty remains regarding the precision of these manually filled fields, but the results of the matching with S2M ROS events (Sect. 4.2.2) indicate overall good data quality. This selection step in the RTM-DB is necessary prior to coupling with S2M, as the coincidence of an RTM natural hazard event with a meteorological ROS event does not, in itself, establish a causal relationship.

The matching between meteorological ROS events from S2M and RTM natural hazard events caused by ROS, was performed over the 2001–2024 period. This coincides with the period when RTM reporting became systematic, allowing use of event counts and ensuring higher data quality. Only RTM events with a precise day-level date were considered. RTM events were assigned to S2M massifs using the centroid of their geographical site, i.e. the (potentially spatially extended) area associated with each event (Sect. 2.4). Elevation was not taken into account, as the centroid elevation is not always representative of the area contributing to the event (e.g., a watershed for torrential floods). A few events located near massif boundaries were manually reassigned to better match the corresponding watershed. RTM events falling outside the S2M massif coverage were disregarded; this concerns only 16 events out of 709 caused by ROS (2 %). Thus, the area covered by S2M massifs corresponds very well to the RTM zones of interest. Matching is performed based on the S2M ROS events. For each S2M ROS event, if at least one RTM event identified as caused by ROS occurred within the same massif on day d or d+1, the ROS event is classified as impactful. Elevation bands are treated independently. After matching, a single RTM event can correspond to multiple ROS events across the different elevation bands of a massif. To present the characteristics (frequency, total rainfall, duration) of impactful events, only the ROS event within the elevation band with the highest total rainfall is retained. This choice aims to best distinguish impactful ROS events from other ROS events, while accounting for the potential extent of the contributing watershed.

3.4 Heavy-Rainfall ROS Event Definition

Impactful ROS events provide an overview of the risks associated with ROS over the 2001–2024 period. Due to the temporal bias in the RTM-DB, they cannot be used to assess long-term trends directly. To overcome this limitation, we first analyze how the proportion of impactful ROS events varies with increasing thresholds based on total rainfall per event and event duration. This allows us to identify criteria that distinguish events more likely to produce impacts, which are then applied to the full 1958–2024 period to investigate their temporal evolution.

Thresholds are initially examined as functions of both total rainfall per event and event duration. As shown in the results (Sect. 4.2.2-3), total rainfall per event alone provides the most reliable criterion, and the threshold at which 50 % of selected ROS are impactful is chosen as it is easy to interpret. This corresponds to a rainfall threshold of 76 mm. There is thus a 50-50

https://doi.org/10.5194/egusphere-2026-2497
Preprint. Discussion started: 26 June 2026

chance that a ROS event exceeding 76 mm of total rainfall will trigger an impact. Events exceeding 76 mm of total rainfall are hereafter referred to as heavy-rainfall ROS events.

3.5 Trend Calculation

Trends are calculated both for ROS events and for heavy rainfall ROS events. They are evaluated quantitatively by comparing mean values between the first and last 30-year periods, namely 1959–1988 and 1995–2024. The snow year, defined from 1 August yyyy to 31 July yyyy+1, is associated with the year yyyy+1. This 30-year window was chosen following the World Meteorological Organization's convention for defining the average climate. The p-value is obtained using a resampling approach: the 60 annual values are randomly permuted (without replacement), and the mean difference is recalculated 1000 times. The resulting p-value represents the probability of obtaining a difference greater than the observed one in absolute value in a stationary framework. We reject the hypothesis of a change between the two periods if the p-value is greater than 5 %.

4 Results

4.1 Comparison with Observation Stations

To assess the representativeness of the characterization of ROS events using S2M, which aggregates data at the massif scale, compared to actual local ROS events, a comparison was made between the results obtained from stations and those obtained from S2M. Each observation station was assigned to the corresponding S2M massif and elevation band based on its location. Since snow observations are largely unavailable at stations, only rainfall data (inferred from precipitation and air temperature data, Sect. 2.3) from the stations were used, while snow presence was derived from S2M to identify ROS events. Because station observations are partly assimilated into S2M, this comparison does not constitute an independent validation. It provides a sensitivity analysis of how ROS characteristics differ when considering precipitation at the local (point) scale versus the massif-averaged scale represented by S2M.

Among the 109 selected observation stations, considering each year independently, 1327 annual data sets were obtained between 1985 and 2023. Each data set includes the number, mean total rainfall per event, and mean duration of ROS events during a snow season. Mean total rainfall and duration were only computed when at least five ROS events occurred in a given year to avoid biases from small sample, resulting in 392 usable data sets. These station-based estimates were then compared to the corresponding S2M values.

A strong consistency is found for the number of ROS events, with a correlation coefficient of $R^2 = 0.77$ (Fig. 3a). The mean relative deviation is 5.8 %. The mean bias error (MBE) of S2M is -0.2 events (-4.6 %), and the root mean square error (RMSE) is 1.9. The S2M ROS occurrence is slightly lower than at the stations. Differences are larger for mean total rainfall and event duration ($R^2 = 0.36$ and 0.30, Fig. 3b–c). The mean relative deviation for total rainfall is 22.5 %, with a negligible MBE of +0.2 mm (+1.4 %) and an RMSE of 5.3 mm. For duration, the mean relative deviation is 22.3 %, with an MBE of +1.77 h (+10.0 %) and an RMSE of 4.9 h. Event duration is generally higher in S2M, while differences in total rainfall

https://doi.org/10.5194/egusphere-2026-2497
Preprint. Discussion started: 26 June 2026

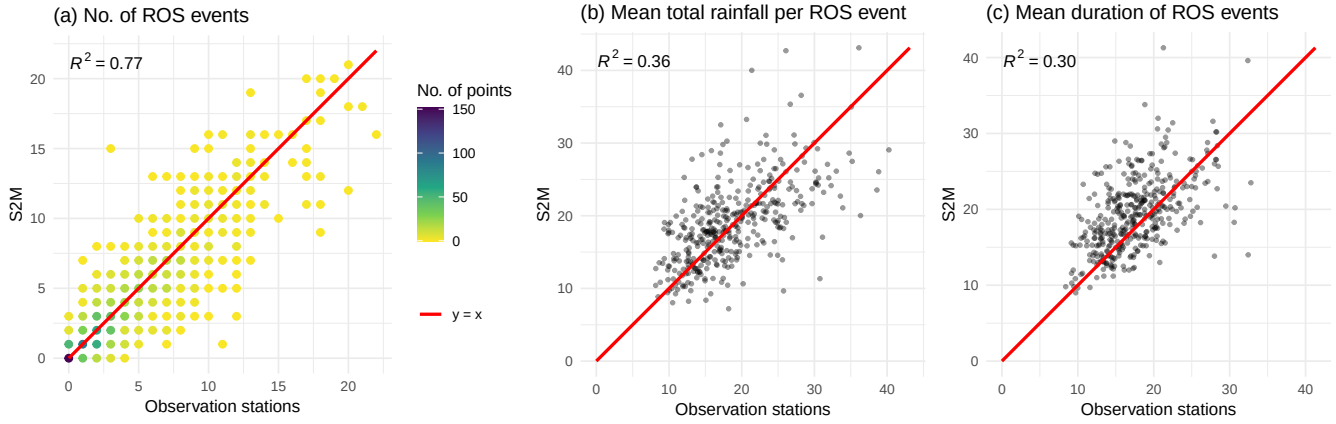

Figure 3. Comparison of S2M with observation stations for (a) number of ROS events, (b) mean total rainfall per ROS event and (c) mean duration of ROS events. Each point corresponds to a year for a given station. In panel (a) points overlap and are therefore colored according to their density.

remain comparatively small in terms of bias. These differences primarily reflect the intrinsic scale mismatch between point observations and massif-scale averages. Local precipitation can occur over short durations, whereas spatial averaging over a massif integrates events that may propagate in space, resulting in longer durations. Overall, the comparison indicates that the main conclusions drawn from S2M are broadly consistent with those obtained from local observations, particularly regarding the number of events and the mean total rainfall per event.

Temporal biases were also examined by analyzing residuals (S2M – station) over time. No significant temporal trends were found for the number or mean total rainfall of events, suggesting that the corresponding trends derived from S2M (Sect. 4.3) are robust. In contrast, event duration exhibits a marked temporal bias, with underestimation before the mid-1990s and overestimation thereafter. This is likely due to improved assimilation of hourly observations from that period onward. As a result, trends in duration are considered unreliable and are not presented.

4.2 Analysis of ROS Events in the French Alps

4.2.1 All ROS Events

Over the 1958–2024 period, an average of 5.5 ROS events occur each year in the French Alps. A strong spatial variability is observed between mountain ranges (Fig. 4a), with a minimum average of 2.2 events in the Queyras and a maximum of 10.2 events in the Chartreuse. A clear pattern emerges, showing a contrast between the northwestern Alps, much more exposed to ROS, and the southeastern Alps. To better understand this distribution, rain events and precipitation events were also analyzed. These were defined in the same way as ROS events, except without the snow cover condition – and, in the case of precipitation events, without distinguishing between liquid and solid phases. The spatial variability of ROS events follows that of rain events

https://doi.org/10.5194/egusphere-2026-2497
Preprint. Discussion started: 26 June 2026

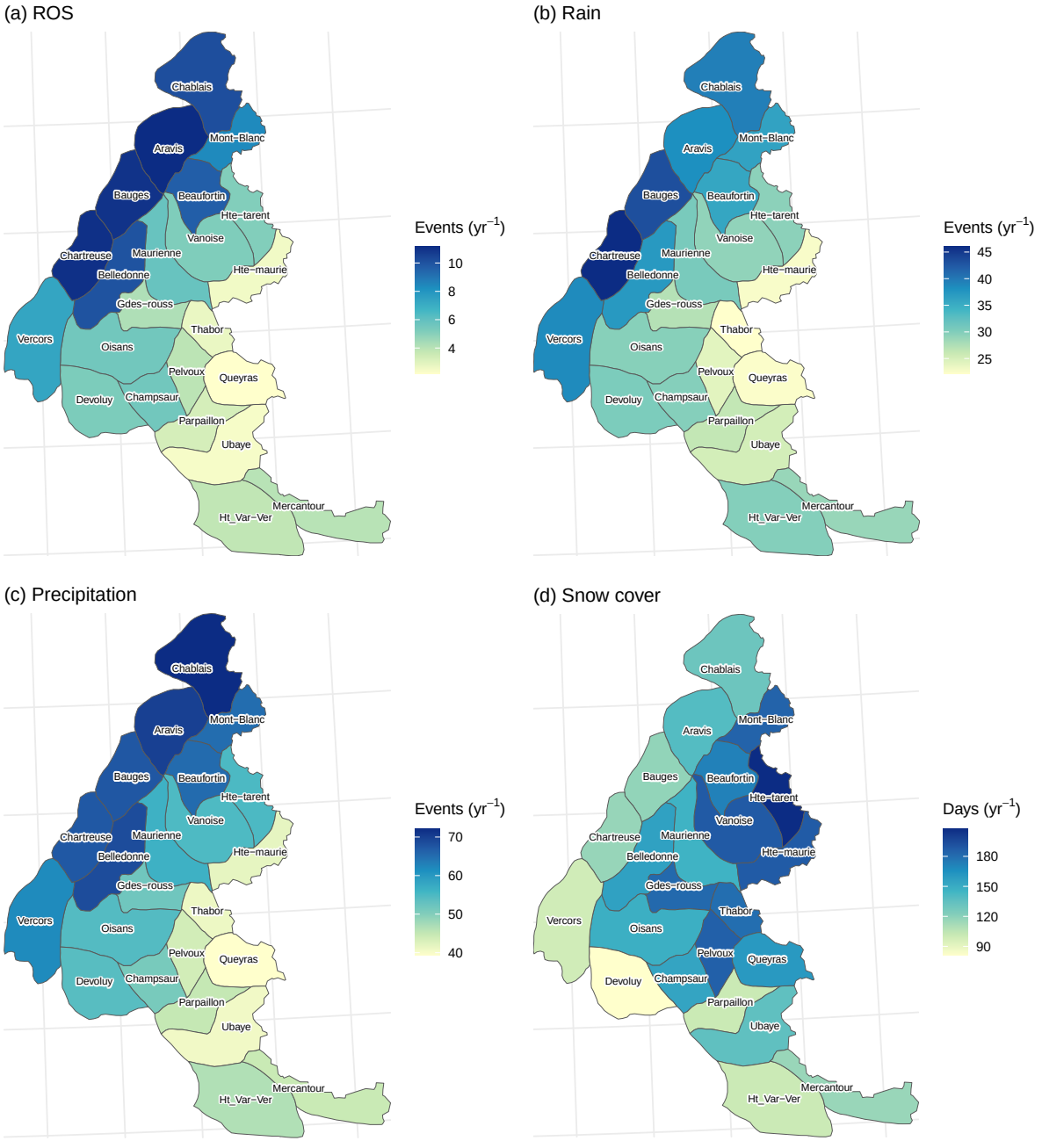

Figure 4. Numbers of (a) ROS events, (b) rain events, (c) precipitation events and (d) snow cover days ($SD \geq 10$ cm and $SWE \geq 10$ mm), per massif, averaged over the 1958–2024 period.

https://doi.org/10.5194/egusphere-2026-2497
Preprint. Discussion started: 26 June 2026

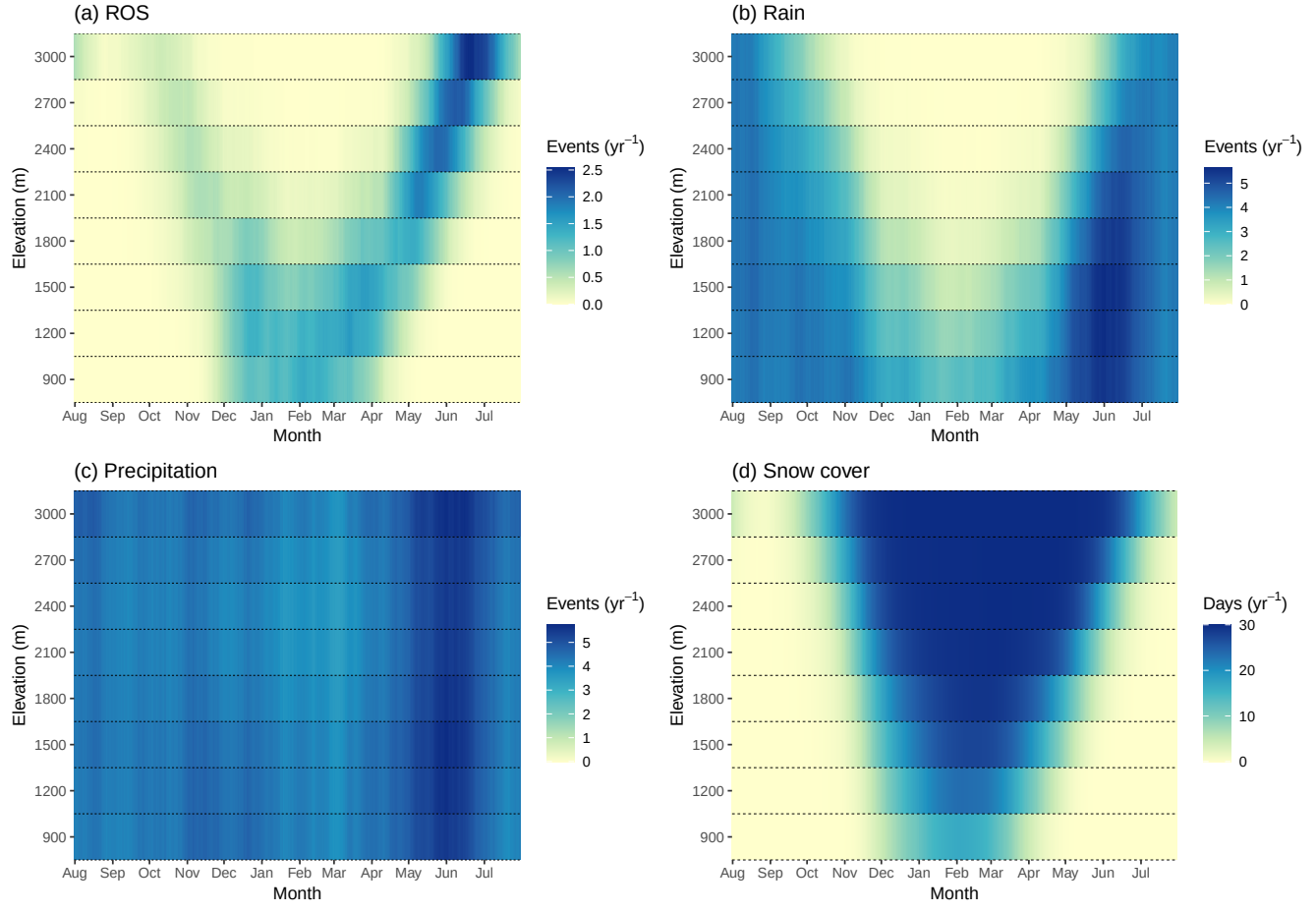

Figure 5. Numbers of (a) ROS events, (b) rain events, (c) precipitation events and (d) snow cover days ($SD \geq 10$ cm and $SWE \geq 10$ mm), per 30-day window and elevation band, averaged over the 1958–2024 period.

(Fig. 4b) and precipitation events (Fig. 4c), although with a stronger relative contrast. In contrast, spatially averaged snow cover follows a distinct spatial pattern primarily controlled by elevation differences between massifs, with the highest massifs (Fig. 1a) exhibiting the longest snow cover duration.

A second source of variability arises from elevation bands. The number of ROS events reaches its maximum at mid-elevations, with 6.2 events per year at 1200 m and 6.5 events at 1500 m. Other elevation bands range between 4.8 and 5.7 events per year on average. Thus, the vertical variability in annual ROS frequency is much weaker than the spatial variability. The elevation bands differ mainly in the seasonality of ROS occurrence. It is therefore useful to examine the distribution as a function of both day of year and elevation, as done by Morán-Tejeda et al. (2016). Figure 5a highlights a distinct V-shaped coupling between season and elevation. At first glance, most ROS events appear to occur at high elevations between May and July. However, as discussed in Sect. 3.2, all elevation bands do not represent the same surface area. When the two highest bands –

https://doi.org/10.5194/egusphere-2026-2497
Preprint. Discussion started: 26 June 2026

whose spatial extent is limited – are disregarded, ROS in the French Alps primarily occurs from early December to early April between 900 m and 1500 m, and in May–June between 2100 m and 2400 m. To better understand the mechanisms behind this coupling and to anticipate possible trends, similar diagrams were produced for rain events (Fig. 5b), precipitation events (Fig. 5c) and snow cover (Fig. 5d). Whereas precipitation events are roughly homogeneous over elevations and seasons, rain events and snow cover exhibit triangular patterns, reflecting a logical complementarity between rain and snow. The V-shaped pattern of ROS corresponds to the edges of this triangle – i.e. the transition periods of snow cover. In mid-winter, liquid precipitation is thus the limiting factor, whereas snow cover becomes limiting during the rest of the year.

The median total rainfall per ROS event across the French Alps is 13 mm (first quartile Q_1 = 8 mm, third quartile Q_3 = 24 mm), with a high standard deviation of 17 mm and a mean of 19 mm. Comparing massif averages reveals a spatial pattern: inner Alpine ranges experience smaller total rainfalls per event than outer ranges (Fig. C1, Appendix C). The minimum mean total rainfall per event is 15 mm in the Grandes Rousses, while the maximum is 25 mm in the Mercantour. The median duration of ROS events is 13 h (Q_1 = 8 h, Q_3 = 19 h), with a high standard deviation of 11 h and a mean of 15 h. No clear spatial pattern emerges, with massif averages ranging between 14 h and 17 h. While the elevation variability is very small for total rainfall per event (minimum and maximum averages of 18.7 mm and 19.5 mm), it is strongly marked for duration: from 19.5 h at 900 m down to 12.7 h at 3000 m, showing a nearly linear decrease with elevation, R^2 = 0.97 (Fig. C2, Appendix C). This dependence of duration on elevation is absent for precipitation events but appears for rain events. At higher elevations, rain (and thus ROS) events are shorter, likely due to more frequent rain–snow phase transitions. With similar total rainfalls but shorter durations, high-elevation ROS events are, therefore, more intense.

4.2.2 Impactful ROS events

A total of 1031 T/I/G events (torrential floods, floods, and landslides) were identified as caused by ROS over the 1958–2024 period in the selection step in RTM-DB (Sect. 3.3). They represent 9.8 % of all T/I/G events during this time span. This proportion is similar across event types, with 9.7 %, 11.6 %, and 9.5 % for T, I, and G respectively. At the annual scale, ROS is thus not a major driver of natural hazard events in mountain areas. However, as shown in Fig. 6a, ROS is an important contributor to winter events, accounting for more than 30 % of all T/I/G events in December. In quantitative terms (Fig. 6b), two distinct periods stand out for RTM ROS-related events: December–January and May–June.

The matching between meteorological ROS events from S2M and RTM natural hazard events caused by ROS over the 2001-2024 period indicates good data quality from the RTM-DB and selection accuracy, as 653 out of 693 RTM events caused by ROS identified in the massifs (94 %) have a corresponding S2M ROS event. This corresponds to an average of 0.33 impactful events per year and per massif, representing 7.2 % of the number of ROS events for the same period. The spatial distribution of impactful ROS events as identified from the RTM-DB (Fig. 7) is mainly consistent with the spatial pattern of all ROS events (Fig. 4a). However, compared to Fig. 4a, the Maurienne and Oisans are more significantly affected, with average values of 0.91 and 0.65 impactful ROS events per year, respectively. This is reflected in the proportion of impactful ROS events, at 19.3 % and 15.2 %. In contrast, the Mercantour massif stands out with zero impactful ROS events recorded between 2001 and 2024.

https://doi.org/10.5194/egusphere-2026-2497
Preprint. Discussion started: 26 June 2026

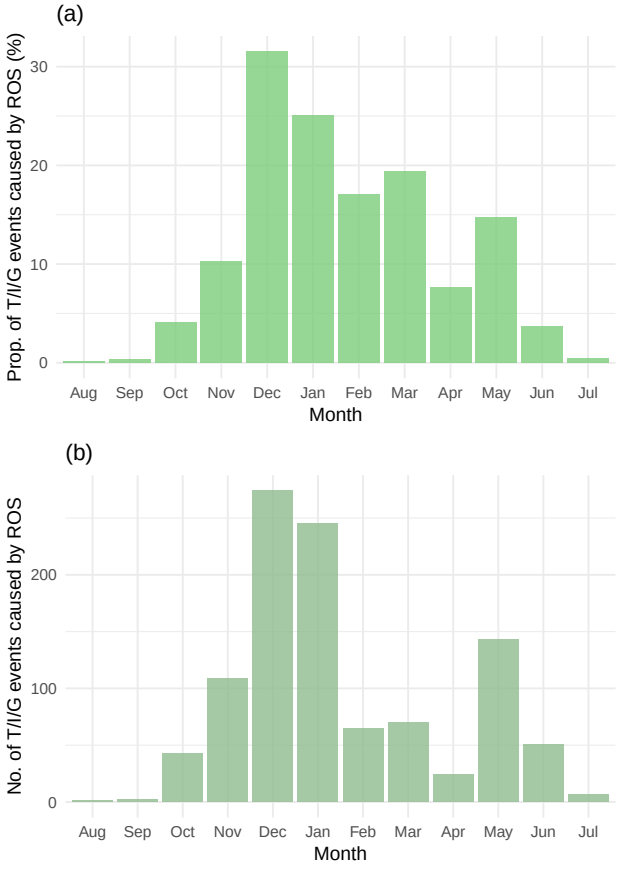

Figure 6. (a) Proportion and (b) number of RTM T/I/G events (torrential floods, floods, and landslides) caused by ROS over the 1958-2024 period.

Impactful ROS events are characterized by significantly higher total rainfalls and longer durations than the complete set of ROS events, as shown by the boxplots in Fig. 8. The median total rainfall per impactful ROS event is 56 mm (Q_1 = 32 mm, Q_3 = 89 mm), corresponding to the 95.3 $\%$ quantile of all ROS events, with a standard deviation of 37 mm. The median duration is 36 hours (Q_1 = 21 h, Q_3 = 55 h), corresponding to the 92.9 $\%$ quantile, with a standard deviation of 22 h. Although the distributions of total rainfall and duration clearly differ between impactful events and all ROS events, these criteria are not sufficient to fully discriminate the impactful behaviour of each event. Impactful ROS events exhibit considerable variability, as shown by the large standard deviations. While most of them exceed the third quartile of total rainfall and duration for all ROS events, some fall well below even the first quartile (Fig. 8). Of the two variables, total rainfall is the more discriminating, with its median corresponding to a higher overall quantile than that of duration.

Figure 9 inspects the proportion of impactful events by applying thresholds to the ROS event variables. Figure 9a is obtained with combined thresholds on both rainfall and duration. Contour lines identify the threshold values needed to reach 25 $\%$,

https://doi.org/10.5194/egusphere-2026-2497
Preprint. Discussion started: 26 June 2026

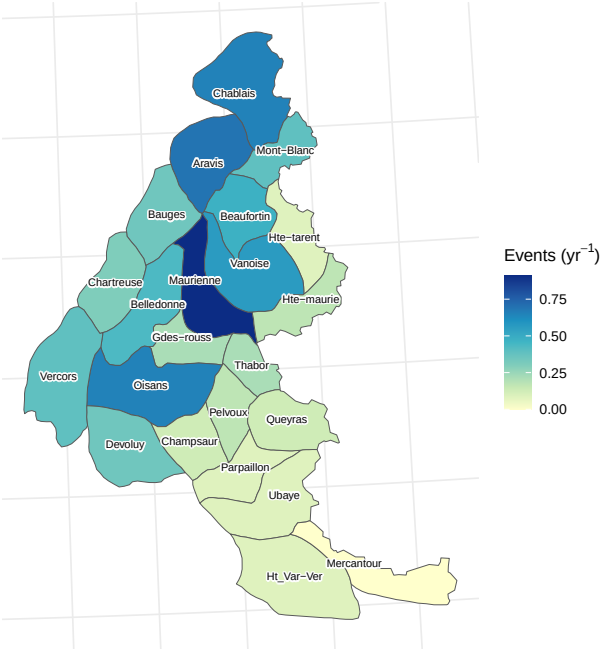

Figure 7. Number of impactful ROS events per massif, averaged over the 2001–2024 period.

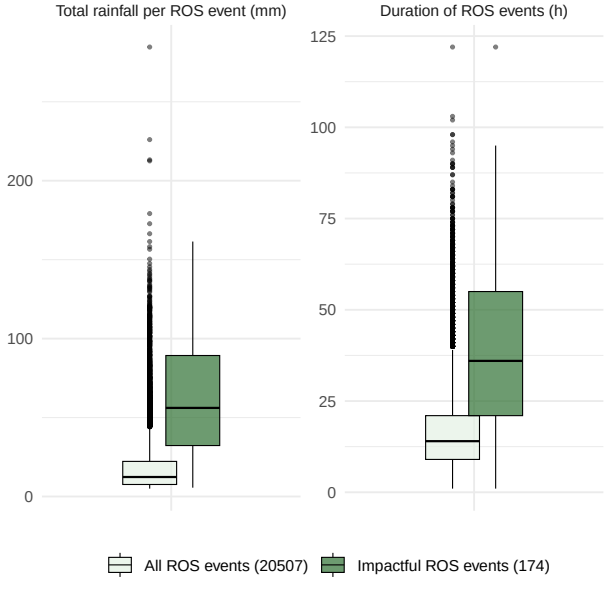

Figure 8. Boxplots of total rainfall and duration per ROS event considering all events or restricting to impactful ones, over the 2001–2024 period.

https://doi.org/10.5194/egusphere-2026-2497
Preprint. Discussion started: 26 June 2026

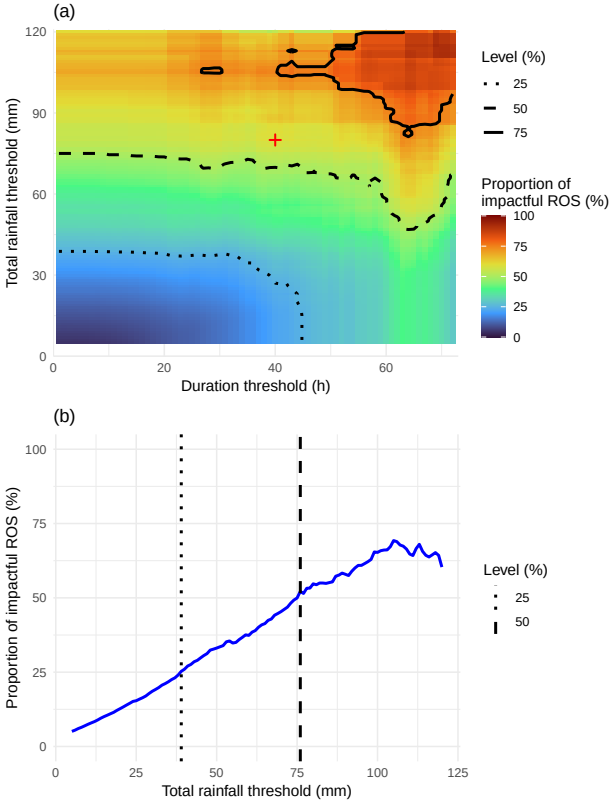

Figure 9. Proportion of impactful ROS events among the ROS events exceeding thresholds.
(a) Thresholds on rainfall and duration. The x- and y-axes represent the applied duration and rainfall thresholds, respectively. The color scale indicates the resulting proportion, with contour lines drawn for reference. The red cross stands as an example: when applying a rainfall threshold of 80 mm and a duration threshold of 40 h, 59 % of the retained ROS events are impactful.
(b) Threshold on rainfall only, corresponding to the vertical line at x = 0 in panel (a).

50 %, or 75 % of impactful events. It confirms that total rainfall is the most discriminating variable, as the 25 % and 50 % contour lines are mostly parallel to the x-axis. The duration threshold has roughly no effect on the proportion of impactful events below about 35 h. However, only events lasting more than 40 h can reach the threshold of 75 % probability of impacts (Fig. 9a). Figure 9a also shows that for high total rainfalls (around 100 mm), longer-lasting events are more likely to result in impacts, since the proportion of impactful ROS events increases when the duration threshold is raised.

4.2.3 Heavy-Rainfall ROS events

Ultimately, as announced in the method (Sect. 3.4), only total rainfall is retained for defining a threshold able to discriminate potentially impactful ROS events with a purely meterological criterion allowing to investigate temporal trends. S2M exhibits a temporal bias in event durations (Sect. 4.1), preventing the use of a criterion based on the duration of ROS events. The heavy-

https://doi.org/10.5194/egusphere-2026-2497
Preprint. Discussion started: 26 June 2026

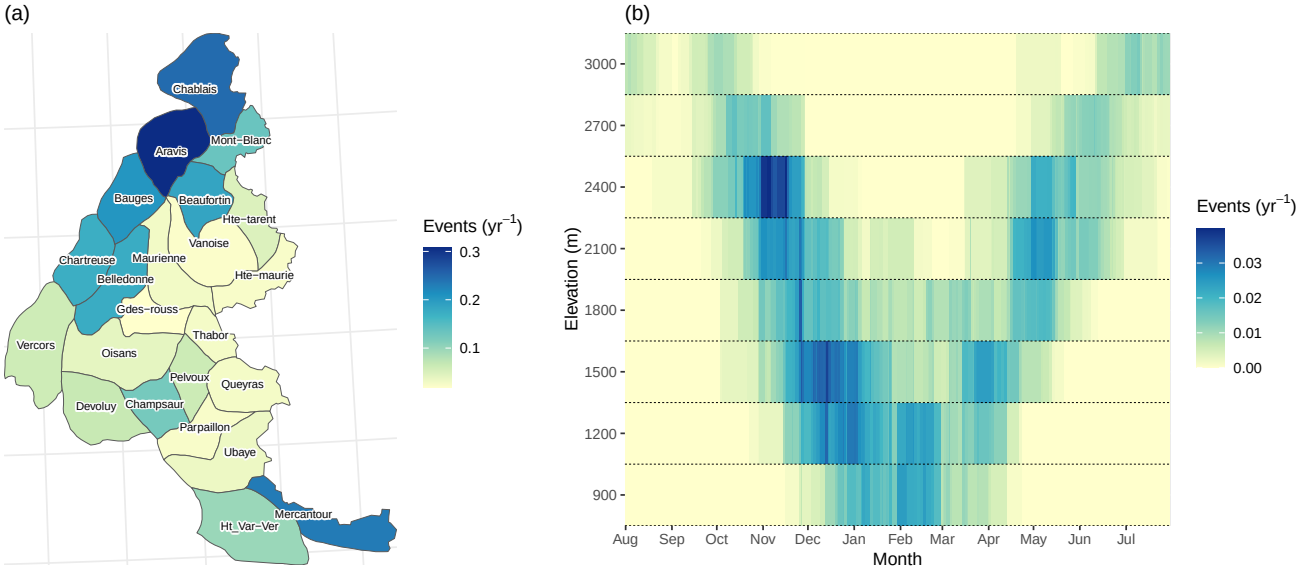

Figure 10. Number of heavy-rainfall ROS events, (a) per massif, and (b) per 30-day window and elevation band, averaged over the 1958–2024 period.

rainfall threshold defined at the 50 % proportion level of impactful ROS events corresponds to 76 mm (98.1 % quantile). This choice is supported by the behaviour observed in Fig. 9b. The proportion of impactful events increases nearly linearly with total rainfall up to about 50 %, whereas beyond this level, the additional gains become progressively smaller. Selecting the 50 % level, therefore, represents a balanced compromise between interpretability and efficiency. This threshold lies above the median total rainfall of impactful events, meaning that over half of them are excluded by the threshold. The available data do not allow for a criterion that is both exclusive of non-impactful events and inclusive of all impactful events. Although it is defined based on the 2001–2024 data, the threshold is applied over the entire 1958–2024 period, assuming that the hydrological response to such events has not substantially changed before 2001.

Over the 1958–2024 period, the French Alps have seen an average of 0.09 heavy-rainfall ROS events per year. Their spatial variability (Fig. 10a) is similar to that of all ROS events (Fig. 4a), with a clear distinction between the outer and inner massifs. However, the distribution of these events by day of year and elevation (Fig. 10b) reveals a different pattern than that for all ROS events (Fig. 5a). While the highest frequency for all ROS events occurs in the late snow season (March–June), heavy-rainfall ROS events are much more concentrated in the early snow season (December–January). This is consistent with higher mean total rainfalls observed in December–January compared to March–June. The dominance of December–January aligns with the peak in RTM events caused by ROS observed earlier (Fig. 6a). November also stands out in the heavy-rainfall ROS event series at 2400 m elevation band, although it was not highlighted in the RTM data set. This is due to a temporal shift in natural hazard seasonality – November was more affected before 2001, when RTM event reporting was not yet systematic. Conversely, May–June, prominent in the RTM data set in number of events (Fig. 6a), do not stand out as much in heavy-rainfall ROS events

https://doi.org/10.5194/egusphere-2026-2497
Preprint. Discussion started: 26 June 2026

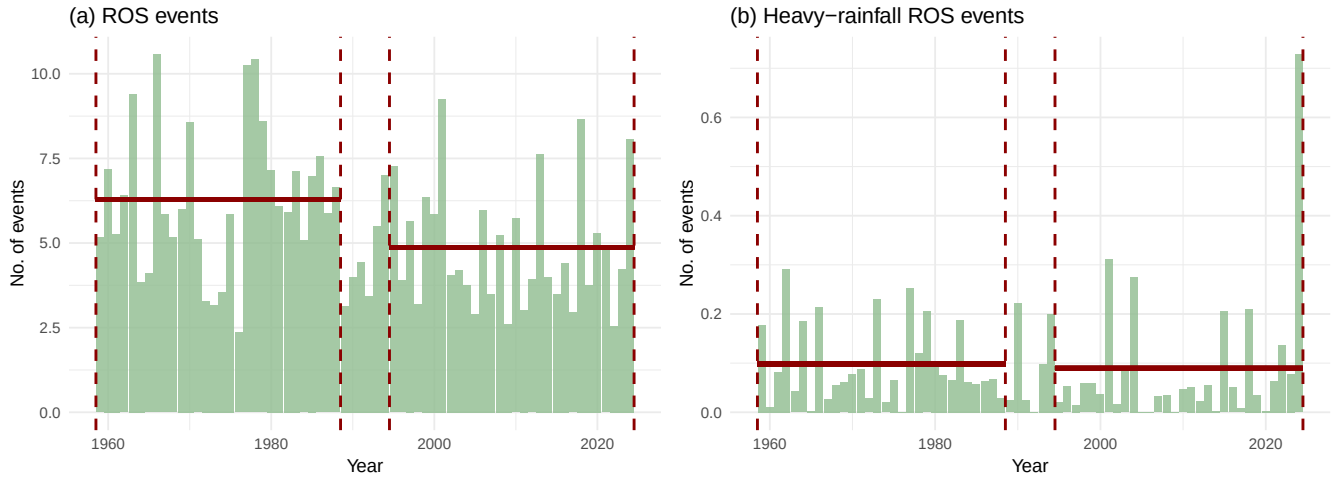

Figure 11. Numbers of (a) ROS events and (b) heavy-rainfall ROS events, per year. Means over the 1959–1988 and 1995–2024 periods. Panels (a) and (b) do not share the same scale.

(Fig. 10b). This means that the heavy-rainfall criterion used to distinguish impactful ROS events is less appropriate for spring and early summer, as the correspondence is weaker than during the winter months.

4.3 Trends in ROS Events (1958–2024)

4.3.1 All ROS Events

In the French Alps, between 1959–1988 and 1995–2024, the number of ROS events per year decreased from 6.29 to 4.88, corresponding to a highly significant relative decrease of 22 % (p_{value} = 0.008). The strong interannual variability, evidenced by the time series in Fig. 11, highlights the relevance of a non-parametric trend assessment, as well as the importance of averaging over sufficiently long periods to obtain a robust result. All mountain ranges follow this downward trend (Fig. 12a) but to varying extents: from -3 % in Mont-Blanc to -44 % in Queyras. For 15 out of 23 massifs, the difference between the two 30-year periods is statistically significant.

These trends vary seasonally, as shown in the plot by day of year and elevation (Fig. 13a). The decrease is concentrated in the second half of the "V-shaped" pattern; that is, toward the end of the snow season. Between early March and late July, the relative decrease is -35 %. A few significant increases are observed between early December and mid-January in the elevation bands from 1500 m to 2100 m (Fig. 13a). Over this portion of the pattern, the relative increase is +18 %. However, this increase remains small in absolute value and does not compensate for the spring–summer decline. It is still noteworthy, as it indicates the emergence of ROS events during a season and at elevations where they were either absent or less frequent in the past.

To understand the origin of these ROS trends, similar analyses were performed for rain events, precipitation events and snow cover (Fig 11b-c-d and Fig 12b-c-d). The spring–summer decline in ROS events coincides with a significant reduction in snow

https://doi.org/10.5194/egusphere-2026-2497
Preprint. Discussion started: 26 June 2026

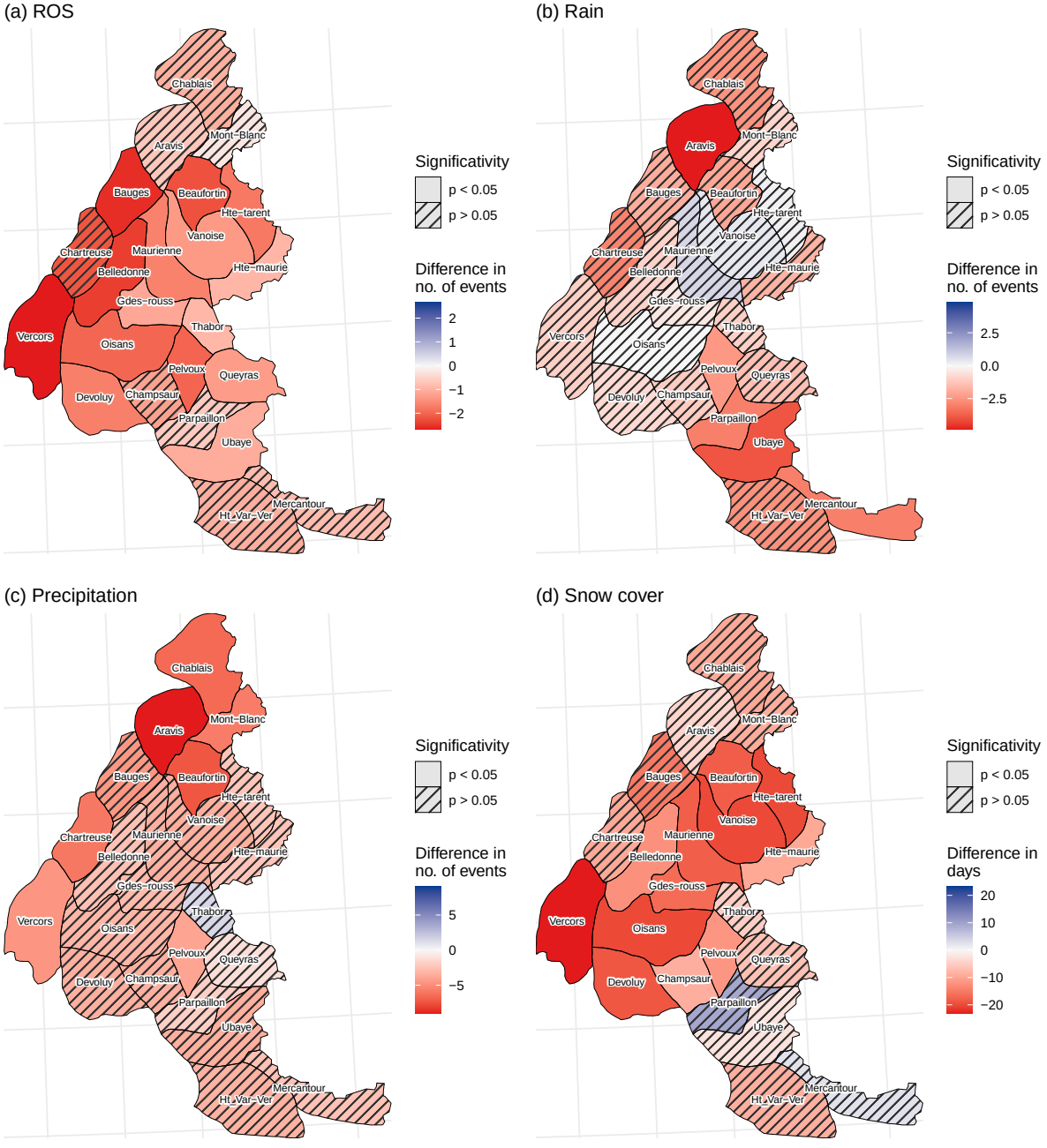

Figure 12. Trends in numbers of (a) ROS events, (b) rain events, (c) precipitation events and (d) snow cover days ($SD \geq 10$ cm and $SWE \geq 10$ mm), per massif. Differences between the 1959–1988 and 1995–2024 periods.

https://doi.org/10.5194/egusphere-2026-2497
Preprint. Discussion started: 26 June 2026

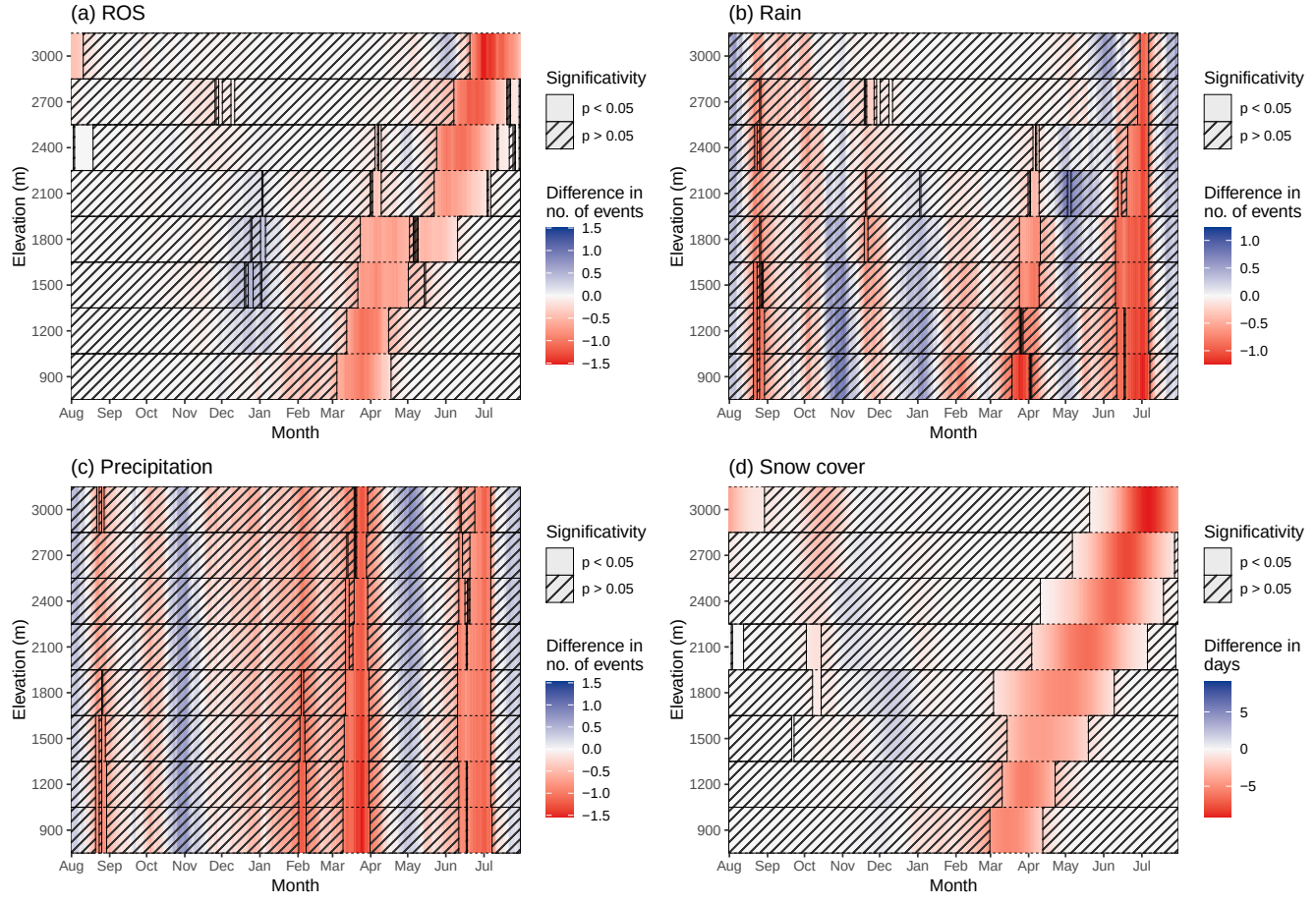

Figure 13. Trends in numbers of (a) ROS events, (b) rain events, (c) precipitation events and (d) snow cover days ($SD \geq 10$ cm and $SWE \geq 10$ mm), per 30-day window and elevation band. Differences between the 1959–1988 and 1995–2024 periods.

cover (Fig. 13d). Between early March and late July, average snow cover across the elevation bands decreased from 76 to 66 days, i.e. -13 % between the two 30-year periods. Over the same period of the year, significant trends are also observed for rain events – decreasing in late March and early July (Fig. 13b) closely matching precipitation events (Fig. 13c) – but overall, there is only a slight, non-significant decrease in the number of rain events (-6 %). Therefore, the spring–summer decrease in ROS events can be attributed to the shortening of the snow season. The increase in ROS events between early December and mid-January in the 1500–2100 m elevation bands, on the other hand, coincides with an increase in the number of rain events (Fig. 13b). Over this part of the year, between 900 and 2400 m, the number of rain events increases by 10 % (though not significantly). No corresponding trend is seen for snow cover (a negligible increase of 2 %). Thus, the increase in ROS events between early December and mid-January can be attributed to the rise in rain events.

https://doi.org/10.5194/egusphere-2026-2497
Preprint. Discussion started: 26 June 2026

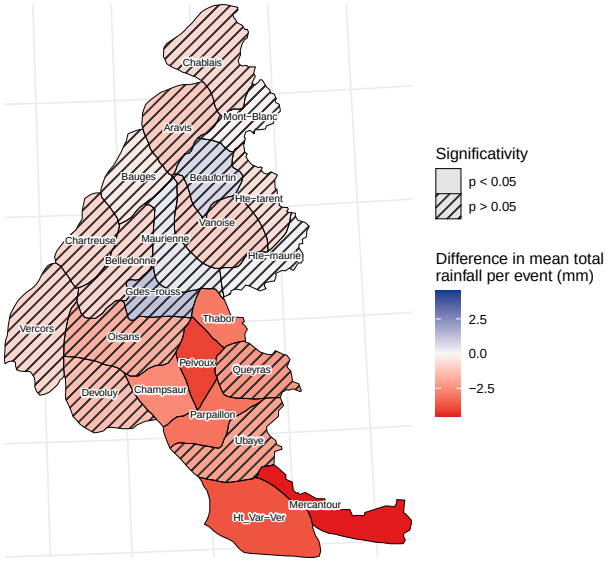

Figure 14. Trends in mean total rainfall per ROS event, per massif, differences between the the 1959–1988 and 1995–2024 periods.

These trends should be considered in the context of a significant overall 7 % decrease in precipitation events at the annual scale. However, this decrease remains much smaller than the 22 % decline observed for ROS events. Conversely, the trend for precipitation events reinforces the importance of the observed increase in ROS between early December and mid-January in the 900–2400 m band. Over that interval, precipitation events decreased by 9 %, while rain events increased by 10 %. These contrasting trends between precipitation and rain events also appear in the spatial patterns of Fig. 12: whereas all massifs except Thabor show a decrease in precipitation events (Fig. 12c), a few massifs, such as Maurienne and Vanoise, exhibit increasing rainfall (Fig. 12b).

Regarding the mean total rainfall per ROS event, a slight non-significant decrease of 0.9 mm (about -5 %) is observed in the French Alps. Trends in mean total rainfall per event do not vary by elevation. The overall decrease is driven by significant declines in the southern Alps (Fig. 14), primarily from February to May. In the eight southern massifs (Thabor, Pelvoux, Champsaur, and below) and over these months, the mean total rainfall per ROS event decreased from 19 mm to 13 mm (-30 %). This decrease is also observed in rain events, but with a smaller magnitude: -15 % in mean total rainfall per event. The spatial pattern in trends also partly applies to rain events, although only the Pelvoux and Mercantour massifs show significant declines.

https://doi.org/10.5194/egusphere-2026-2497
Preprint. Discussion started: 26 June 2026

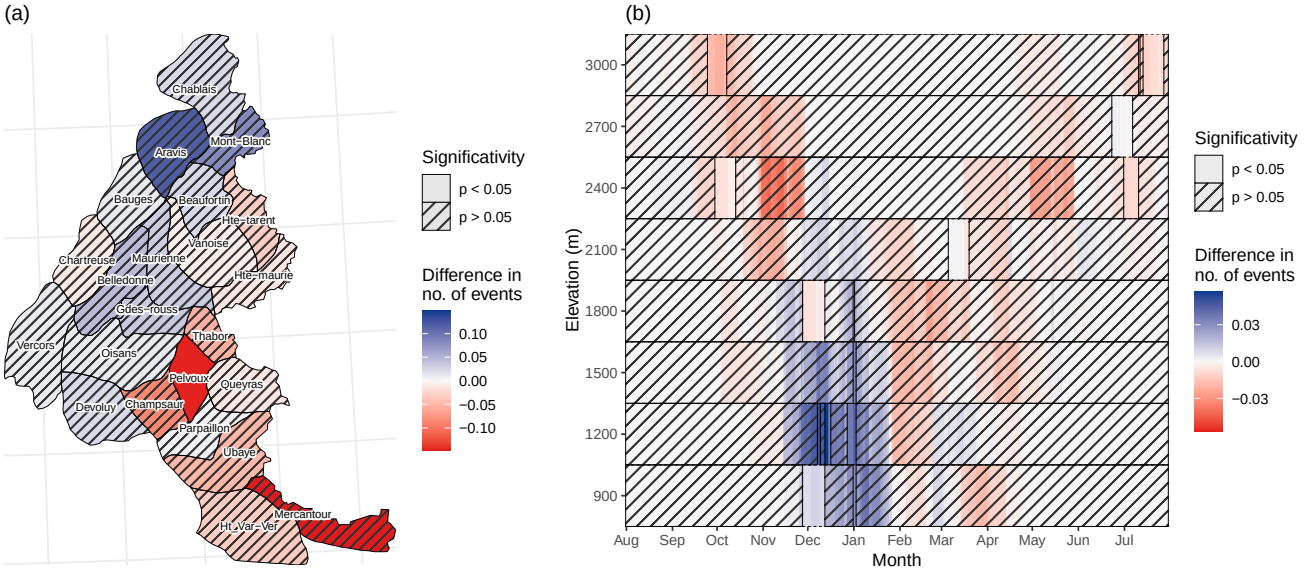

Figure 15. Trends in number of heavy-rainfall ROS events, (a) per massif, and (b) per 30-day window and elevation band. Differences between the 1959–1988 and 1995–2024 periods.

4.3.2 Heavy-Rainfall ROS Events

The number of heavy-rainfall ROS events shows a decreasing trend of -9 % between the 1959–1988 and 1995–2024 periods, smaller than the -22 % observed for all ROS events, indicating that the proportion of heavy-rainfall ROS events has increased over time. This decrease is not statistically significant, but the small sample size of events exceeding the heavy-rainfall threshold (76 mm), representing on average only 0.09 events per year compared to 5.5 events per year for all ROS events (Sect. 4.2.1), makes it difficult to detect significant trends. The small sample size also leads to an even stronger interannual variability than that for all ROS events (Fig. 11b). Notably, Figure 11b shows that the 2024 snow year (1 August 2023 to 31 July 2024) was truly exceptional, with a record number of heavy-rainfall ROS events, in part due to a large spatial extent of individual meteorological events affecting several massifs. This is consistent with several ROS-triggered torrential floods, such as those in the Hautes-Alpes department on 1 December 2023 (Département des Hautes-Alpes, 2024) and the flooding of the Étançons torrent on 21 June 2024 (Blanc et al., 2024).

Unlike the general decrease observed for all ROS events (Fig. 12a), the trend in the number of heavy-rainfall ROS events is not spatially uniform (Fig. 15a). A clear contrast emerges between the external massifs, mostly located in the northern Alps, which show increases, and the internal massifs, mainly in the southern Alps, which show decreases. This spatial pattern mirrors the trends in mean total rainfall per event (Fig. 14).

Trends in heavy-rainfall ROS events also vary with season and elevation (Fig. 15b). Notably, the most significant trends are positive, occurring mainly in December. The seasonal pattern of these trends is similar to that observed for all ROS events

https://doi.org/10.5194/egusphere-2026-2497
Preprint. Discussion started: 26 June 2026

(Fig. 13a): an increase from early December to mid-January, while the rest of the year shows a predominance of negative trends. Trends were also examined for precipitation events and rain events exceeding the heavy-rainfall threshold (not shown). The comparison highlights two main drivers in December–January. First, the observed increase is associated with a rise in precipitation events exceeding the threshold. This increase is specific to heavy-precipitation events, as the number of all precipitation events shows a 9 % decrease for these months (Sect. 4.3.1). Thus, both the frequency and proportion of extremes in precipitation have increased during this part of the year. Second, the relative changes differ markedly between types of events: +16 % (+0.063 events) for heavy-precipitation events, +43 % (+0.020 events) for heavy-rainfall events, and +133 % (+0.027 events) for heavy-rainfall ROS events. The amplification of the relative trend from precipitation to rainfall, despite a smaller change in absolute numbers, suggests an additional influence from rising temperatures, which favors a liquid rather than a solid precipitation phase. When comparing rainfall and ROS, the higher positive trend for ROS in both relative and absolute terms indicates that heavy-rainfall events have increasingly translated into heavy-rainfall ROS events in the recent period. Conversely, warming leads to a shorter snow season, which limits the occurrence of heavy-rainfall ROS events in spring and summer, even though the number of rain events exceeding the rainfall threshold increases over the same period. These trends represent a major shift in the seasonality of heavy-rainfall ROS events. While they mainly occurred in October–November and May during the 1959–1988 period, they now predominantly take place in December–January. This seasonal shift is accompanied by a downward shift in elevation: events were previously most frequent in the 2100 m and 2400 m bands, whereas they now mainly affect lower elevations, from the 900 m to 1500 m bands.

5 Discussion

5.1 Occurrence and trends

The occurrence characteristics of ROS events identified in this study are consistent with findings reported in the literature. Most studies conducted at mid-latitudes highlight two main occurrence regimes: winter at lower elevations and late spring to early summer at higher elevations (McCabe et al., 2007; Morán-Tejeda et al., 2016). The study most comparable to ours in terms of both geography and methodology is that of Morán-Tejeda et al. (2016) for Switzerland. While Morán-Tejeda et al. (2016) identify two distinct clusters in day-of-year versus elevation graphs, the season–elevation coupling in our results (Fig. 5a) appears much more linear. This difference may stem from the exhaustiveness of the S2M reanalysis used here, which provides uniform coverage across all elevation bands. In contrast, Morán-Tejeda et al. (2016) relied on observation stations, which do not allow for homogeneous elevation coverage.

Regarding trends, the two main components observed here – a decrease in ROS occurrence in spring–summer and an increase in winter (Sect. 4.3.1) – have already been documented at mid-latitudes (Freudiger et al., 2014; Beniston and Stoffel, 2016; Morán-Tejeda et al., 2016; Pall et al., 2019). However, the winter increase at higher elevations – between 1500 m and 3000m depending on the article – reported in the literature (McCabe et al., 2007; Beniston and Stoffel, 2016; Musselman et al., 2018; Bonsoms et al., 2024) is only partially observed in our results, and is essentially confined to the period between early December

https://doi.org/10.5194/egusphere-2026-2497
Preprint. Discussion started: 26 June 2026

and mid-January (Fig. 13a). This discrepancy may be explained by the overall decrease in precipitation events in the French Alps over the 1958–2024 study period (Sect. 4.3.1).

The decrease in ROS occurrence in spring and the increase in winter are consistent with a warming climate (Morán-Tejeda et al., 2016; Pall et al., 2019), and its known consequences on precipitation phase and alpine snow cover. Indeed, rising temperatures lead to an increasing proportion of precipitation falling as rain, as illustrated by our results and consistent with the conclusions of Bozzoli et al. (2024). The combined effect of reduced snowfall and warmer conditions favouring melting leads to a significant decrease in snow cover duration of between -3 and -8 days per decade, as reported by several authors based on various datasets (highly supervised snow observatories, Essery et al. (2020), large networks of snow observation stations, Matiu et al. (2021), several land surface reanalyses, Monteiro and Morin (2023), or optical satellite imagery, Barrou Dumont et al. (2025)). This decrease in snow cover duration is mainly attributed to an earlier snowmelt in spring (Dumont et al., 2025), which was found to be the main driver of the reduction of ROS events in our study.

The contrast in trends between all ROS events and heavy-rainfall ROS events is also reflected in previous studies. For example, Morán-Tejeda et al. (2016) report a slight overall decrease for all ROS events in Switzerland, whereas Beniston and Stoffel (2016) find a 40 % increase in heavy-rainfall ROS events (> 50 mm) above 1000 m between 1960 and 2015. Nevertheless, our results show that, at the scale of the French Alps, heavy-rainfall ROS events have decreased overall (Sect. 4.3.2), although this trend exhibits strong spatial contrasts (Fig. 15a).

5.2 Spatial Patterns of ROS Climatology and Trends

The massif-based analysis highlights strong spatial contrasts across the French Alps. A clear distinction emerges between the northwestern part of the range, which is more exposed to ROS events and to precipitation in general, and the southeastern massifs (Fig. 4a). This pattern can be explained by Atlantic circulation regimes, which tend to generate precipitation over the first mountain ranges encountered by incoming air masses (Blanchet et al., 2021). These Atlantic flows are sometimes associated with warm-air intrusions, which favor ROS conditions, thereby explaining why the relative contrast between massifs is stronger for ROS events than for rain or precipitation events alone (Fig. 4b-c). Atmospheric influences also help explain the spatial differences in trends. For mean total rainfall per event (Fig. 14), the decreases observed in the southern massifs coincide with the retreat of Mediterranean influence during winter and spring in the southern Alps over the past 60 years (Blanchet et al., 2021). Under these conditions, warm-air intrusions leading to ROS events are more frequently associated with Atlantic flows, which primarily affect the northern Alps and yield lower total rainfall in the southern massifs. The same explanation related to the weakening Mediterranean influence (Blanchet et al., 2021) can be invoked to account for the spatial pattern of trends in heavy-rainfall ROS events (Fig. 15a), as these are intrinsically linked to trends in total rainfall per event.

5.3 Impacts

Results on impactful ROS events highlight strong spatial variability, with some massifs being far more prone to natural hazard events than others (Fig. 7). Certain areas are indeed more susceptible due to a combination of factors such as topography, geology, and the drainage network. This is notably the case for the Maurienne massif, which is characterized by steep slopes

https://doi.org/10.5194/egusphere-2026-2497
Preprint. Discussion started: 26 June 2026

and highly degraded terrains that favor debris flows (Martin-Cocher, 1984). As a result, lower total rainfall can be sufficient to trigger hazardous processes in this region. This result also demonstrates the potential of the RTM-DB for future works to look for region-dependent thresholds of weather warning procedures accounting for these variable observed impacts. However, this spatial variability may also partly reflect biases in the RTM-DB. The Maurienne and Oisans massifs, which record the largest number of impactful ROS events (Sect. 4.2.2), are characterized by high population density and significant economic assets, particularly winter sports resorts. In contrast, the Mercantour massif, where no impactful ROS events were identified, is sparsely populated. The apparent absence of impactful events there is therefore very likely not due to a lack of natural phenomena, but rather to a lack of impacts and, consequently, of reporting in the RTM-DB.

The impact-based threshold analysis shows that, for a given rainfall total, the probability of impacts increases with increasing ROS event duration (Fig. 9a). This result may appear counter-intuitive, as longer events are associated with lower rainfall intensities. However, it is consistent with the findings of Würzer et al. (2016), who showed that the snowpack dampens the hydrological response to short and intense events, while amplifying the response to long-lasting events. A plausible explanation is that longer events allow a greater amount of snowmelt driven by a positive surface energy balance, mainly explained by a high sensible heat flux, substantially increasing the total runoff. Indeed, previous works have shown that snowmelt is strongly driven by sensible heat fluxes during ROS events (Corripio and López-Moreno, 2017; Bonsoms et al., 2024).

For heavy-rainfall ROS events, results partially agree with the conclusions of Würzer et al. (2016) for the Swiss Alps. That study showed that most potentially impactful ROS events occur above 2000 m, toward the end of the melt season in spring–summer and in late autumn (Würzer et al., 2016). This pattern was attributed to higher precipitation totals and larger total runoff at higher elevations (Sui and Koehler, 2001; Katz et al., 2023). While we also find a concentration of heavy-rainfall ROS events in late autumn, their occurrence is lower in spring–summer, and these events are also frequent at elevations below 2000 m (Fig. 10b). In addition, the observed trends indicate a shift in the elevation range of heavy-rainfall ROS events toward the 900 m to 1500 m bands (Sect. 4.3.2). These lower elevations are more densely populated and host more human infrastructure than the 2100 m and 2400 m bands that were previously affected. As a result, heavy-rainfall ROS events occurring today might be more impactful.

5.4 Limits of the study

The use of reanalysis data is both a major strength and a limitation of this study. It provides high temporal resolution and consistent spatial coverage, a level of detail rarely matched in previous studies, but also introduces uncertainties inherent to model-based products. The comparison against observation stations (Sect. 4.1) showed that the aggregation of results by massif and elevation band is representative of in situ observations, but potential errors, particularly in snow-related variables, remain difficult to quantify.

The hourly S2M product is obtained through temporal interpolation of original data available at variable temporal resolutions (6 h for the large scale meteorological guess, 1 h for automatic weather stations, but only daily for numerous precipitation observations and old records of minimum and maximum air temperatures). Prior to the 1990s, when hourly observations were unavailable, assessing the quality of this interpolation is difficult. In addition, the spatial density of observations is also highly

https://doi.org/10.5194/egusphere-2026-2497
Preprint. Discussion started: 26 June 2026

variable over time. Time-dependent biases may therefore exist, as illustrated by Vernay et al. (2022) for air temperatures. In this study, a previously undocumented issue was emphasized in this dataset concerning the duration of precipitation events, which is underestimated before the 1990s and overestimated afterwards, resulting in an inconsistent trend on that criterion (Sect. 4.1). This limitation should be considered for other applications of the S2M dataset that are sensitive to this criterion.

Besides, the hourly temporal resolution used in this study requires caution when comparing results with earlier studies based on daily data. However, most identified ROS events have sub-daily durations (Sect. 4.2.1), and the methodology enforces a minimum separation of 12 h between consecutive events (Sect. 3.1). Thus, event counts should be close to those derived from a daily time step, making comparison with the existing literature still meaningful.

The systematic event-based analysis across massifs and elevation bands provides unprecedented spatial and temporal coverage, but it does not allow for a hydrological assessment. Heavy-rainfall ROS events should therefore be interpreted as an *indirect* proxy for potential impacts. Previous studies using hydrological models have highlighted the importance of additional variables, such as snowpack liquid water content and density, for flood hazard assessment (Würzer et al., 2016; Katz et al., 2023). Snowpack conditions are particularly critical, as snowmelt can account for up to 30 $\%$ of the total runoff during major flood events (Rössler et al., 2014; Blanc et al., 2024).

6 Conclusions

This study delivers the first systematic, high-resolution climatology of ROS events for the French Alps. It links meteorological ROS detected using the S2M reanalysis with an impact database (RTM-DB). This coupling is a main methodological advance in terms of ROS investigations: we explicitly distinguish between all ROS events and those associated with documented natural-hazard impacts. Our main findings are threefold. First, ROS occurrence displays strong spatial and elevation variability: ROS events are more frequent in north-western massifs than in south-eastern ones, and seasonality depends markedly on elevation (winter prevalence at low elevations, spring–summer at higher elevations). Second, impactful ROS events are clearly associated with larger total rainfall per event and longer durations. A heavy-rainfall threshold of 76 mm (50 $\%$ impact probability) provides a simple, interpretable discriminator of impact-prone events. Third, trend analysis reveals a substantial overall decline in ROS frequency (-22 $\%$ between 1959–1988 and 1995–2024), concentrated in spring–summer, while December–January shows increases in the 1500–2100 m elevation bands consistent with more frequent rain occurrences. Heavy-rainfall ROS events exhibit a smaller decline (-9 $\%$) and have shifted toward lower, more populated elevations, which could result in more impacts.

In summary, this work establishes a comprehensive climatological and impact-oriented baseline for ROS in the French Alps. It demonstrates the value of combining high-resolution meteorological reanalysis with impact inventories and opens avenues to improve the tools dedicated to operational hazard assessment and risk-reduction strategies. Future work could extend this study toward more event-based hydrological analyses. Approaches at the watershed scale would help refine the understanding of runoff generation and improve the physical interpretation of ROS-related impacts.

https://doi.org/10.5194/egusphere-2026-2497
Preprint. Discussion started: 26 June 2026

Data availability. S2M data sets are freely available for download at https://doi.org/10.25326/37#v2024.1. Observation data and long-term homogenized series from Météo-France are also freely available, as part of the French government's open data initiative, at https://meteo.data.gouv.fr/datasets. The RTM event database and observation data from EDF stations are proprietary.

Appendix A: Homogenization of Air Temperature Time Series from Stations

Air temperature time series at observation stations were homogenized using the *Standard Normal Homogeneity Test* (SNHT; Alexandersson (1986)), by comparison with the Météo-France long-term homogenized series (LSH). These LSH are monthly time series of mean $TNTX$, where $TNTX$ is defined as the daily mean temperature computed as the average of daily minimum and maximum air temperatures. The LSH are statistically corrected for inhomogeneities and constitute the reference data set recommended by Météo-France for assessing climate change in France. For each station, monthly series of mean $TNTX$, denoted X_t, were derived from hourly observations. The geographically closest LSH reference series, denoted R_t, was then selected. The SNHT was applied to the difference series $(X - R)_t$. The normalized series is defined as:

$Z_t = \dfrac{(X-R)_t - \mu}{\sigma}$, where μ and σ are the mean and standard deviation of $(X - R)_t$.

For each potential break point k, the means before and after k are:

$$\overline{Z}_1(k) = \frac{1}{k}\sum_{t=1}^{k} Z_t, \qquad \overline{Z}_2(k) = \frac{1}{N-k}\sum_{t=k+1}^{N} Z_t,$$

and the SNHT statistic is:

$$T_k = k\,\overline{Z}_1(k)^2 + (N-k)\,\overline{Z}_2(k)^2.$$

The test statistic is defined as $T = \max_{1\le k\le N} T_k$. For a given confidence level α, a critical value T_{crit} is used to assess homogeneity: if $T > T_{crit}$, the series is considered inhomogeneous, and a break is detected at the value of k maximizing T_k. The procedure is applied iteratively to each resulting sub-period. For each segment, the temperature is corrected to X'_t so that the mean of $(X' - R)_t$ over the segment equals μ. These corrections are then applied to the original hourly temperature series. The following parameters were used for the iterative detection:

- confidence level: $\alpha = 80\ \%$;
- maximum number of break points: 5;
- minimum spacing between two break points: 12 months.

Appendix B: Criterion for precipitation phase identification based on temperature

ROS events derived from observation stations strongly depend on the criterion used to determine the precipitation phase. To avoid introducing a bias in the validation related to precipitation phase partitioning, the same criterion as in S2M must be

https://doi.org/10.5194/egusphere-2026-2497
Preprint. Discussion started: 26 June 2026

applied to the observations. However, S2M corrects the precipitation phase as a function of the resulting snow cover, using observations from snow stations (Vernay et al., 2022). It is therefore not possible to apply exactly the same method to observational data sets. A temperature-based criterion that best reproduces the rain–snow discrimination automatically performed by S2M must thus be identified. It is done by comparing the original S2M version with modified versions in which the precipitation phase is determined using different temperature-based criteria. The comparison focuses on ROS events through the annual number of events, the mean total rainfall per event, and the mean event duration for each massif and elevation band. Let P denote total precipitation and RF total liquid precipitation – i.e. total rainfall. Two types of temperature-based criteria are considered:

- Temperature threshold T_s:

  If $T < T_s : RF = 0$

  If $T \geq T_s : RF = P$

- Temperature-based sigmoid between T_1 and T_2:

  If $T < T_1 : RF = 0$

  If $T > T_2 : RF = P$

  If $T_1 \leq T \leq T_2 : RF = sigm(T)\,P \quad \text{with } sigm(T) = \dfrac{1}{1+\exp\left(-k\left(T - \frac{T_1+T_2}{2}\right)\right)} \quad \text{where } k = \dfrac{10}{T_2 - T_1}.$

According to Table B1, the temperature criterion that best reproduces the S2M rain–snow discrimination is a threshold of $T_s = 0.9$ °C. This criterion yields the lowest root mean square errors for all three variables. Mean bias errors are among the lowest as well, with a very slight overestimation corresponding to -2.2 % for the number of events, -0.7 % for the mean total rainfall per event, and -1.1 % for the mean event duration. As S2M provides a binary distinction between solid and liquid precipitation, it is consistent that a threshold-based criterion performs better than a fractional partitioning using a sigmoid function. Sigmoid-based criteria perform particularly poorly for event duration, which is strongly overestimated. For events whose duration would otherwise be limited by decreasing temperatures and a transition from rain to snow, the sigmoid formulation continues to assign small but non-zero rainfall amounts, artificially extending the event duration as long as the threshold of 3 mm over 12 h is exceeded.

https://doi.org/10.5194/egusphere-2026-2497
Preprint. Discussion started: 26 June 2026

Table B1. Comparison between S2M and modified versions using a temperature-based rain–snow discrimination criterion. The number (N), mean total rainfall (RF in mm), and mean duration (Δt in h) of ROS events are compared for each year, for each massif and elevation band. Results are summarized using the mean bias error (MBE) and the root mean square error (RMSE). Best-performing values are highlighted in bold.

	Criterion	MBE			RMSE		
		N	RF	Δt	N	RF	Δt
Threshold	0.5 °C	1.41	1.06	0.46	2.09	3.15	2.15
	0.6 °C	1.15	0.87	0.33	1.81	2.85	1.98
	0.7 °C	0.91	0.62	0.18	1.54	2.51	1.81
	0.8 °C	0.65	0.42	**0.07**	1.27	2.14	1.62
	0.9 °C	-0.13	-0.13	-0.17	**0.44**	**0.91**	**0.88**
	1.0 °C	-0.16	-0.16	-0.20	0.49	0.98	0.96
	1.1 °C	-0.33	-0.35	-0.32	0.73	1.50	1.28
	1.2 °C	-0.51	-0.54	-0.45	0.95	1.93	1.55
Sigmoid	-2.0 °C to 4.0 °C	0.61	-1.35	3.57	1.40	2.82	4.51
	-1.0 °C to 3.0 °C	0.30	-0.80	3.00	1.07	2.19	3.85
	-0.5 °C to 2.5 °C	0.16	-0.53	2.56	0.92	1.90	3.37
	-0.5 °C to 2.0 °C	0.77	**0.12**	2.51	1.42	2.27	3.45
	0.0 °C to 2.0 °C	**0.04**	-0.30	1.98	0.79	1.64	2.75
	0.0 °C to 1.5 °C	0.70	0.35	1.83	1.33	2.22	2.79
	0.0 °C to 1.0 °C	1.39	1.04	1.63	2.07	3.16	2.85
	0.5 °C to 1.5 °C	-0.09	-0.15	1.19	0.66	1.33	1.92
	0.5 °C to 1.0 °C	0.74	0.52	0.80	1.37	2.31	2.01

https://doi.org/10.5194/egusphere-2026-2497
Preprint. Discussion started: 26 June 2026

Appendix C: Supplementary Figures

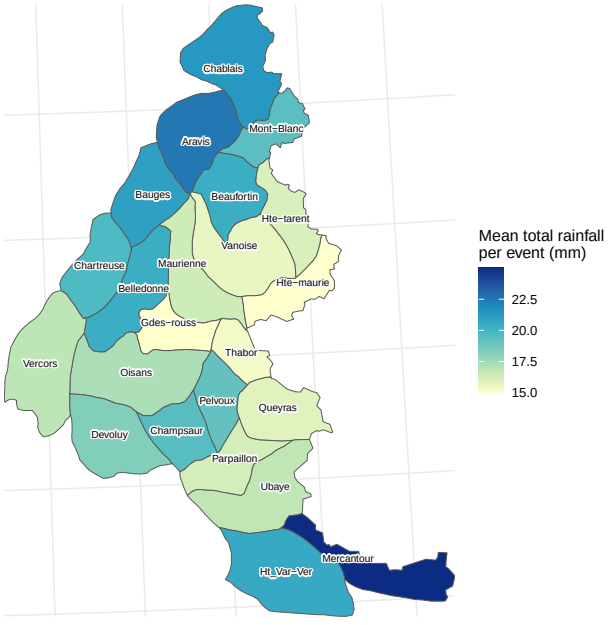

Figure C1. Mean total rainfall per ROS event, per massif, averaged over the 1958–2024 period.

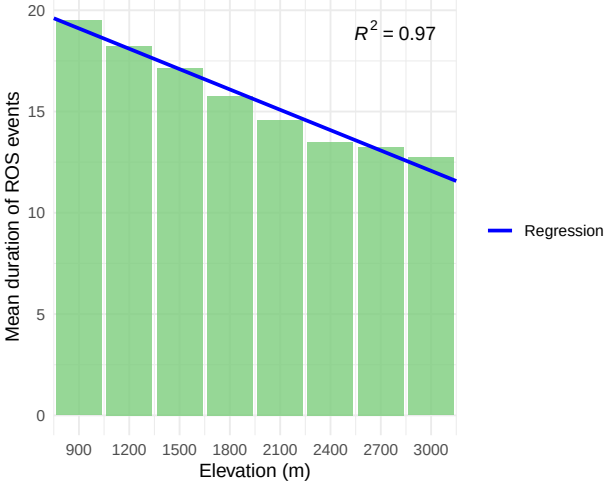

Figure C2. Mean duration of ROS events per elevation band, averaged over the 1958–2024 period, and linear regression.

https://doi.org/10.5194/egusphere-2026-2497
Preprint. Discussion started: 26 June 2026

Author contributions. Paul Fournier conducted the study under the supervision of Antoine Blanc and Juliette Blanchet. Paul Fournier wrote the manuscript, with review and editing by Antoine Blanc, Juliette Blanchet and Matthieu Lafaysse. Matthieu Lafaysse provided expertise on S2M and contributed to the discussion.

Competing interests. The authors declare that they do not have any competing interests.

Acknowledgements. This paper is the result of strong cooperation between the RTM service of the National Forest Office (ONF) and the *Institut des Géosciences de l'Environnement* (IGE, Institute of Environmental Geosciences). We are grateful to Météo-France and *Électricité de France* (EDF) for their help, advice, and participation in work meetings. Large language models were used to translate some expressions from French to English and to rephrase parts of the manuscript.

Financial support. This work was conducted as part of a research internship funded by the RTM service of the National Forest Office (ONF).

https://doi.org/10.5194/egusphere-2026-2497
Preprint. Discussion started: 26 June 2026

References

Alexandersson, H.: A homogeneity test applied to precipitation data, Journal of Climatology, 6, 661–675, https://doi.org/10.1002/joc.3370060607, 1986.

Barrou Dumont, Z., Gascoin, S., Inglada, J., Dietz, A., Köhler, J., Lafaysse, M., Monteiro, D., Carmagnola, C., Bayle, A., Dedieu, J.-P., Hagolle, O., and Choler, P.: Trends in the annual snow melt-out day over the French Alps and Pyrenees from 38 years of high-resolution satellite data (1986–2023), The Cryosphere, 19, 2407–2429, https://doi.org/10.5194/tc-19-2407-2025, 2025.

Beniston, M. and Stoffel, M.: Rain-on-snow events, floods and climate change in the Alps: Events may increase with warming up to 4 °C and decrease thereafter, Science of The Total Environment, 571, 228–236, https://doi.org/10.1016/j.scitotenv.2016.07.146, 2016.

Bisquert, A., Mainieri, R., Carladous, S., Robert, Y., Giacona, F., Verry, P., and Eckert, N.: La base de données événementielles RTM pour la connaissance des risques naturels en montagne : L'exemple du département de l'Isère (France), Journal of Alpine Research | Revue de géographie alpine, https://doi.org/10.4000/137kf, 2025.

Blanc, A., Misset, C., Mainieri, R., and Llamas, B.: Rétro-analyse de la crue du torrent des Etançons du 21 juin 2024, Tech. rep., ONF-RTM, https://hal.science/hal-04865442, 2024.

Blanchet, J., Creutin, J.-D., and Blanc, A.: Retreating winter and strengthening autumn Mediterranean influence on extreme precipitation in the Southwestern Alps over the last 60 years, Environmental Research Letters, 16, 034 056, https://doi.org/10.1088/1748-9326/abb5cd, 2021.

Bonsoms, J., López-Moreno, J. I., Alonso-González, E., Deschamps-Berger, C., and Oliva, M.: Rain-on-snow responses to warmer Pyrenees: a sensitivity analysis using a physically based snow hydrological model, Natural Hazards and Earth System Sciences, 24, 245–264, https://doi.org/10.5194/nhess-24-245-2024, 2024.

Bozzoli, M., Crespi, A., Matiu, M., Majone, B., Giovannini, L., Zardi, D., Brugnara, Y., Bozzo, A., Berro, D. C., Mercalli, L., and Bertoldi, G.: Long-term snowfall trends and variability in the Alps, International Journal of Climatology, 44, 4571–4591, https://doi.org/10.1002/joc.8597, 2024.

Casellas, E., Bech, J., Veciana, R., Pineda, N., Rigo, T., Miró, J. R., and Sairouni, A.: Surface precipitation phase discrimination in complex terrain, Journal of Hydrology, 592, 125 780, https://doi.org/10.1016/j.jhydrol.2020.125780, 2021.

Cohen, J., Ye, H., and Jones, J.: Trends and variability in rain-on-snow events, Geophysical Research Letters, 42, 7115–7122, https://doi.org/10.1002/2015GL065320, 2015.

Corripio, J. G. and López-Moreno, J. I.: Analysis and Predictability of the Hydrological Response of Mountain Catchments to Heavy Rain on Snow Events: A Case Study in the Spanish Pyrenees, Hydrology, 4, https://doi.org/10.3390/hydrology4020020, 2017.

Creutin, J.-D., Blanchet, J., Reverdy, A., Brochet, A., Lutoff, C., and Robert, Y.: Reported Occurrence of Multiscale Flooding in an Alpine Conurbation over the Long Run (1850–2019), Water, 14, 548, https://doi.org/10.3390/w14040548, 2022.

Dumont, M., Monteiro, D., Filhol, S., Gascoin, S., Marty, C., Hagenmuller, P., Morin, S., Choler, P., and Thuiller, W.: The European Alps in a changing climate: physical trends and impacts, Comptes Rendus. Géoscience, 357, 25–42, https://doi.org/10.5802/crgeos.288, 2025.

Durand, Y., Brun, E., Merindol, L., Guyomarc'h, G., Lesaffre, B., and Martin, E.: A meteorological estimation of relevant parameters for snow models, Annals of Glaciology, 18, 65–71, https://doi.org/10.3189/S0260305500011277, 1993.

Département des Hautes-Alpes: Intempéries de décembre : le Département a répondu présent, https://www.hautes-alpes.fr/actualite/intemperies-de-decembre-le-departement-a-repondu-present/, last access: 23 November 2025, 2024.

https://doi.org/10.5194/egusphere-2026-2497
Preprint. Discussion started: 26 June 2026

Essery, R., Kim, H., Wang, L., Bartlett, P., Boone, A., Brutel-Vuilmet, C., Burke, E., Cuntz, M., Decharme, B., Dutra, E., Fang, X., Gusev, Y., Hagemann, S., Haverd, V., Kontu, A., Krinner, G., Lafaysse, M., Lejeune, Y., Marke, T., Marks, D., Marty, C., Menard, C. B., Nasonova, O., Nitta, T., Pomeroy, J., Schädler, G., Semenov, V., Smirnova, T., Swenson, S., Turkov, D., Wever, N., and Yuan, H.: Snow cover duration trends observed at sites and predicted by multiple models, The Cryosphere, 14, 4687–4698, https://doi.org/10.5194/tc-14-4687-2020, 2020.

Freudiger, D., Kohn, I., Stahl, K., and Weiler, M.: Large-scale analysis of changing frequencies of rain-on-snow events with flood-generation potential, Hydrology and Earth System Sciences, 18, 2695–2709, https://doi.org/10.5194/hess-18-2695-2014, 2014.

Froidurot, S., Zin, I., Hingray, B., and Gautheron, A.: Sensitivity of Precipitation Phase over the Swiss Alps to Different Meteorological Variables, Journal of Hydrometeorology, 15, 685–696, https://doi.org/10.1175/JHM-D-13-073.1, 2014.

Jennings, K. S., Winchell, T. S., Livneh, B., and Molotch, N. P.: Spatial variation of the rain–snow temperature threshold across the Northern Hemisphere, Nature Communications, 9, 1148, https://doi.org/10.1038/s41467-018-03629-7, 2018.

Katz, L., Lewis, G., Krogh, S., Drake, S., Hanan, E., Hatchett, B., and Harpold, A.: Antecedent Snowpack Cold Content Alters the Hydrologic Response to Extreme Rain-on-Snow Events, Journal of Hydrometeorology, 24, https://doi.org/10.1175/JHM-D-22-0090.1, 2023.

Lafaysse, M., Cluzet, B., Dumont, M., Lejeune, Y., Vionnet, V., and Morin, S.: A multiphysical ensemble system of numerical snow modelling, The Cryosphere, 11, 1173–1198, https://doi.org/10.5194/tc-11-1173-2017, 2017.

Li, D., Lettenmaier, D. P., Margulis, S. A., and Andreadis, K.: The Role of Rain-on-Snow in Flooding Over the Conterminous United States, Water Resources Research, 55, 8492–8513, https://doi.org/10.1029/2019WR024950, 2019.

Martin-Cocher, J.: Etude géologique de la stabilité des versants de la rive droite de l'Arc entre Saint-Michel de Maurienne et La Praz (Savoie), Ph.D. thesis, Université Scientifique et Médicale de Grenoble, https://theses.hal.science/tel-00511863, 1984.

Matiu, M., Crespi, A., Bertoldi, G., Carmagnola, C. M., Marty, C., Morin, S., Schöner, W., Cat Berro, D., Chiogna, G., De Gregorio, L., Kotlarski, S., Majone, B., Resch, G., Terzago, S., Valt, M., Beozzo, W., Cianfarra, P., Gouttevin, I., Marcolini, G., Notarnicola, C., Petitta, M., Scherrer, S. C., Strasser, U., Winkler, M., Zebisch, M., Cicogna, A., Cremonini, R., Debernardi, A., Faletto, M., Gaddo, M., Giovannini, L., Mercalli, L., Soubeyroux, J.-M., Sušnik, A., Trenti, A., Urbani, S., and Weilguni, V.: Observed snow depth trends in the European Alps: 1971 to 2019, The Cryosphere, 15, 1343–1382, https://doi.org/10.5194/tc-15-1343-2021, 2021.

McCabe, G. J., Clark, M. P., and Hay, L. E.: Rain-on-Snow Events in the Western United States, Bulletin of the American Meteorological Society, 88, 319–328, https://doi.org/10.1175/BAMS-88-3-319, 2007.

Moisselin, J.-M., Schneider, M., Canellas, C., and Mestre, O.: Les changements climatiques en France au XXe siècle - Étude des longues séries homogénéisées de données de température et de précipitations, La Météorologie, 2002, 45–56, https://doi.org/10.4267/2042/36233, 2002.

Monteiro, D. and Morin, S.: Multi-decadal analysis of past winter temperature, precipitation and snow cover data in the European Alps from reanalyses, climate models and observational datasets, The Cryosphere, 17, 3617–3660, https://doi.org/10.5194/tc-17-3617-2023, 2023.

Morán-Tejeda, E., López-Moreno, J., Stoffel, M., and Beniston, M.: Rain-on-snow events in Switzerland: recent observations and projections for the 21st century, Climate Research, 71, 111–125, https://doi.org/10.3354/cr01435, 2016.

Musselman, K. N., Lehner, F., Ikeda, K., Clark, M. P., Prein, A. F., Liu, C., Barlage, M., and Rasmussen, R.: Projected increases and shifts in rain-on-snow flood risk over western North America, Nature Climate Change, 8, https://doi.org/10.1038/s41558-018-0236-4, 2018.

Pall, P., Tallaksen, L. M., and Stordal, F.: A Climatology of Rain-on-Snow Events for Norway, Journal of Climate, 32, 6995–7016, https://doi.org/10.1175/JCLI-D-18-0529.1, 2019.

https://doi.org/10.5194/egusphere-2026-2497
Preprint. Discussion started: 26 June 2026

Rössler, O., Froidevaux, P., Börst, U., Rickli, R., Martius, O., and Weingartner, R.: Retrospective analysis of a nonforecasted rain-on-snow flood in the Alps – a matter of model limitations or unpredictable nature?, Hydrology and Earth System Sciences, 18, 2265–2285, https://doi.org/10.5194/hess-18-2265-2014, 2014.

Singh, P., Spitzbart, G., Hübl, H., and Weinmeister, H. W.: Hydrological response of snowpack under rain-on-snow events: a field study, Journal of Hydrology, 202, 1–20, https://doi.org/10.1016/S0022-1694(97)00004-8, 1997.

Strizzolo, F., Drouet, A.-S., Ayache, P., Forte, P., and Lorentz, J.: Crue du torrent de Montfort entre Lumbin et Crolles : retour sur la gestion de crise, Institut des Risques Majeurs, https://www.irma-grenoble.com/01actualite/01articles_afficher.php?id_actualite=760, 2023.

Sui, J. and Koehler, G.: Rain-on-snow induced flood events in Southern Germany, Journal of Hydrology, 252, 205–220, https://doi.org/10.1016/S0022-1694(01)00460-7, 2001.

Uppala, S. M., KÅllberg, P. W., Simmons, A. J., Andrae, U., Bechtold, V. D. C., Fiorino, M., Gibson, J. K., Haseler, J., Hernandez, A., Kelly, G. A., Li, X., Onogi, K., Saarinen, S., Sokka, N., Allan, R. P., Andersson, E., Arpe, K., Balmaseda, M. A., Beljaars, A. C. M., Berg, L. V. D., Bidlot, J., Bormann, N., Caires, S., Chevallier, F., Dethof, A., Dragosavac, M., Fisher, M., Fuentes, M., Hagemann, S., Hólm, E., Hoskins, B. J., Isaksen, L., Janssen, P. A. E. M., Jenne, R., Mcnally, A. P., Mahfouf, J.-F., Morcrette, J.-J., Rayner, N. A., Saunders, R. W., Simon, P., Sterl, A., Trenberth, K. E., Untch, A., Vasiljevic, D., Viterbo, P., and Woollen, J.: The ERA-40 re-analysis, Quarterly Journal of the Royal Meteorological Society, 131, 2961–3012, https://doi.org/10.1256/qj.04.176, 2005.

Vernay, M., Lafaysse, M., Monteiro, D., Hagenmuller, P., Nheili, R., Samacoïts, R., Verfaillie, D., and Morin, S.: The S2M meteorological and snow cover reanalysis over the French mountainous areas: description and evaluation (1958–2021), Earth System Science Data, 14, 1707–1733, https://doi.org/10.5194/essd-14-1707-2022, 2022.

Vionnet, V., Brun, E., Morin, S., Boone, A., Faroux, S., Le Moigne, P., Martin, E., and Willemet, J.-M.: The detailed snowpack scheme Crocus and its implementation in SURFEX v7.2, Geoscientific Model Development, 5, 773–791, https://doi.org/10.5194/gmd-5-773-2012, 2012.

World Meteorological Organization: Climate, https://wmo.int/topics/climate, last access: 14 October 2025, 2022.

Würzer, S., Jonas, T., Wever, N., and Lehning, M.: Influence of Initial Snowpack Properties on Runoff Formation during Rain-on-Snow Events, Journal of Hydrometeorology, 17, 1801–1815, https://doi.org/10.1175/JHM-D-15-0181.1, 2016.

Ye, H., Yang, D., and Robinson, D.: Winter rain on snow and its association with air temperature in northern Eurasia, Hydrological Processes, 22, 2728–2736, https://doi.org/10.1002/hyp.7094, 2008.